UCRL-11043

University of California

Ernest O. Lawrence Radiation Laboratory

TWO-WEEK LOAN COPY

This is a Library Circulating Copy which may be borrowed for two weeks. For a personal retention copy, call Tech. Info. Division, Ext. 5545

SOLUBILITY OF HELIUM IN URANIUM DIOXIDE

Berkeley, California

DISCLAIMER

This document was prepared as an account of work sponsored by the United States Government. While this document is believed to contain correct information, neither the United States Government nor any agency thereof, nor the Regents of the University of California, nor any of their employees, makes any warranty, express or implied, or assumes any legal responsibility for the accuracy, completeness, or usefulness of any information, apparatus, product, or process disclosed, or represents that its use would not infringe privately owned rights. Reference herein to any specific commercial product, process, or service by its trade name, trademark, manufacturer, or otherwise, does not necessarily constitute or imply its endorsement, recommendation, or favoring by the United States Government or any agency thereof, or the Regents of the University of California. The views and opinions of authors expressed herein do not necessarily state or reflect those of the United States Government or any agency thereof or the Regents of the University of California.

Research and Development

UCRL-11043

UNIVERSITY OF CALIFORNIA
Lawrence Radiation Laboratory
Berkeley, California

AEC Contract No. W-7405-eng-48

SOLUBILITY OF HELIUM IN URANIUM DIOXIDE

Firooz Rufeh

(M. S. Thesis)

March 19, 1964

Printed in USA. Price $1.50. Available from the
Office of Technical Services
U. S. Department of Commerce
Washington 25, D.C.

SOLUBILITY OF HELIUM IN URANIUM DIOXIDE

Contents

Abstract v

I. Introduction 1

II. Data Analysis 3

III. Experimental Procedure

A. Sample Preparation 6

B. Infusion Stage 6

C. Isotope Dilution Stage 8

IV. Results

A. Data 13

B. Error Analysis 13

C. Validation of Henry's Law 16

D. Effect of Infusion Time 16

E. Temperature Dependence 19

F. Comparison with Bostrom's Experiment 19

G. Conclusions 22

Acknowledgments 26

Appendixes

A. Apparatus 27

1. Infusion System 27

2. Isotope Dilution System 46

B. UO_2 Chemical Certification Report 52

C. Mass Spectrometric Analysis 53

References 54

SOLUBILITY OF HELIUM IN URANIUM DIOXIDE

Firooz Rufeh

Inorganic Materials Research Division,
Lawrence Radiation Laboratory,
and Department of Nuclear Engineering,
University of California, Berkeley, California

March 19, 1964

ABSTRACT

Solubility of helium in uranium dioxide powder at 1200 and 1300°C was found to be 6.71×10^{-4} and 3.23×10^{-4} cc(STP)/g-atm, respectively. From a plot of helium concentration as a function of time, a diffusion coefficient at 1200°C was estimated to be 1.5×10^{-13} cm^2/sec. It was also shown that the He-UO_2 system obeys Henry's law.

A high-pressure furnace that operates at 2000°C in the pressure range of 100 atm to 10^{-5} torr was designed and constructed to saturate UO_2 powder of 4-μ average particle size with He^4. The powder was then dissolved in a fused salt in an induction chamber. The released He^4 was mixed with a known quantity of He^3 and the mixture was analyzed with a mass spectrometer to determine the He^4 - He^3 ratio, hence the original mass of He^4 in the sample.

I. INTRODUCTION

The retention of noble-gas fission products by ceramic fuels is an important criterion in assessing the suitability of a material for reactor applications. At elevated temperature one of the most important release mechanisms is that of lattice diffusion.[1]

The extensive effort that has been devoted to this problem has almost universally emphasized the postirradiation anneal experiment. In this technique the noble gases xenon and krypton are generated within the specimen by fission of the uranium component of the fuel under thermal-neutron irradiation. The specimen is then heated (annealed) and the release of the noble gases is measured as a function of time. The noble-gas solutes which can be studied are limited to xenon and krypton, since the other rare gases are not fission products. The major effort has been directed toward UO_2 as the fuel material,[2-5] although some work has been reported on UC.[6]

Because helium is a noble gas like the practically important xenon and krypton fission products, a study of the diffusional release characteristics of He in UO_2 would be a valuable adjunct to the analogous experiments involving Xe and Kr. This is particularly true since the solute size effect should be quite evident in comparing He and Xe diffusion in the same material. It would be expected that helium would diffuse by an interstitial mechanism, while Kr and Xe diffusion would be governed primarily by vacancy movement.

Because of their large atomic radii compared with the lattice spacing, xenon and krypton are essentially insoluble (in the thermodynamic sense) in UO_2 or UC. The only method of generating significant quantities of these gases in the solid is by fission of uranium.

Since helium is not a fission product it cannot be generated in UO_2 or UC by neutron irradiation. However, because it probably occupies interstitial sites in the solid lattice, helium exhibits a measurable solubility and can be forced into the solid at high pressures ($\approx$ 100 atm).

If helium is introduced into UO_2 or UC by pressurization of the sample in an atmosphere of helium (hereafter called the "infusion" process), there exists a reciprocal connection between the thermodynamics of the system as reflected in the solubility, and the kinetics as represented by the diffusion process. In order to study the diffusion phenomenon the solubility of the gas must be known, since this parameter constitutes one of the boundary conditions on the diffusion equation. If, on the other hand, one sets out to measure the solubility of He in UO_2 or UC, the diffusion phenomena govern the rate of approach to saturation, and, short of waiting an infinite time, the diffusivity is required in order to estimate the fractional saturation in a finite time. In principle, a single set of experiments can be used to measure both the solubility and the diffusivity. In practice, the experimental conditions are usually adjusted such that the measurement of one of these parameters is considerably more precise than the other.

The purpose of this research was to measure the solubility of helium in UO_2, and to investigate the applicability of Henry's law to this system. Small particles ($\approx 4\mu$) of UO_2 were held in helium (50 to 100 atm pressure) for times long enough to insure a close approach to saturation (up to 99%). The samples were then melted with the aid of a flux, and the quantity of released helium was measured. Experiments were conducted at 1200 and 1300°C. By following the approach to saturation, the diffusivity of He in UO_2 could also be estimated, although with considerably less precision than solubility.

A review of the literature revealed only one other study of this system. Bostrom[8] studied the solubility of helium in 0.15-μ particles of UO_2 at 800 and 1000°C and pressures of 0.5 and 1 atm. These data will subsequently be discussed in more detail.

II. DATA ANALYSIS

Since the solubility of He in UO_2 was measured by infusion experiments of finite duration, it is important to know something of the manner in which saturation is approached. In this section we consider the relation between the measured amount of helium in spherical particles of UO_2 and the solubility, diffusivity, and time of infusion.

Diffusion in a sphere is governed by the following differential equation:

$$\frac{\partial C}{\partial t} = D\left(\frac{\partial^2 C}{\partial r^2} + \frac{2}{r}\frac{\partial C}{\partial r}\right), \tag{1}$$

where C is concentration in the solid at time t and radial position r, and D is the diffusion coefficient. The concentration is measured in cubic centimeters of helium at STP per gram of UO_2.

With the initial condition

$$C(r, 0) = 0 \tag{2}$$

and the boundary conditions

$$C(a, t) = C_s, \left(\frac{\partial C}{\partial r}\right)_0 = 0, \tag{3}$$

the solution of Eq. (1) is given by:[7]

$$C(r, t) = C_s\left\{1 - \frac{2a}{\pi r}\sum_{n=1}^{\infty}\frac{(-1)^n}{n}\sin\left(\frac{n\pi r}{a}\right)\exp\left[-\frac{n^2\pi^2 Dt}{a^2}\right]\right\}, \tag{4}$$

where C_s corresponds to the concentration of solute in the sphere at equilibrium and is given by $C_s = kP$; P is the external pressure and k is the Henry's-law constant. The sphere radius is denoted by a.

The average concentration is obtained from Eq. (4), and

$$\overline{C}(t) = \frac{1}{\frac{4\pi a^3}{3}}\int_0^a 4\pi r^2 C(r, t)\, dr. \tag{5}$$

The fractional saturation is defined by

$$f(t) = \frac{\overline{C}(t)}{C_s} . \tag{6}$$

For the sphere this is[7]

$$F(t) = 1 - \frac{6}{\pi^2} \sum_{n=1}^{\infty} \frac{1}{n^2} \exp\left[- \frac{n^2 \pi^2 Dt}{a^2} \right]. \tag{7}$$

Useful asymptotic forms of Eq. (7) are:[7]

$$F(t) = 1 - \frac{6}{\pi^2} \exp\left[- \frac{\pi^2 Dt}{a^2} \right] \qquad \text{long times, } \frac{\pi^2 Dt}{a^2} > 1 \tag{8}$$

and

$$F(t) = \frac{6}{\sqrt{\pi}} \sqrt{\frac{Dt}{a^2}} - 3 \frac{Dt}{a^2} \qquad \text{short times, } \frac{\pi^2 Dt}{a^2} < 1 . \tag{9}$$

At $\pi Dt/a^2 = 1$, the values of $F(t)$, as calculated from Eqs. (8) and (9), are $F(t) = 0.771$ and $F(t) = 0.774$, respectively. The true value corresponding to Eq. (7) lies between these two.

In the experiments reported here the long-time approximation, Eq. (8), is the most useful. The quantity measured is the total amount of helium that has been absorbed per gram of UO_2, or $\overline{C}(t) = C_s F(t)$. As $t \to \infty$, $F(t) \to 1$ and the measurements yield the solubility directly.

For finite diffusion time, however, the quantity absorbed does not correspond to the solubility, and the fractional saturation must be estimated. One method is to use known values of diffusivity and particle diameter and compute $F(t)$ for each experiment from Eq. (8). If the diffusion coefficient is not known it can be estimated by conducting

a few of the experiments at various infusion times and fitting the data according to Eq. (8). The latter approach was followed in this work.

However, most of the experiments reported here involved infusion times sufficiently long such that the deviation of the fractional saturation from unity was considerably less than the precision of the data. In this case the solubility could be obtained directly from the long-time experiments, and the runs at shorter infusion times utilized to estimate the diffusivity by fitting a curve of the form of Eq. (8) to the data.

A separate series of isothermal experiments at a number of infusion times must be carried out at each temperature in order to determine the effect of temperature on C_s and D.

III. EXPERIMENTAL PROCEDURE

A. Sample Preparation

Uranium dioxide powder of 4-μ average diameter was obtained from the Uranium Carbide Nuclear Company, which supplied the following specifications:

Chemical Certification Report

Gram U/gram	0.879830
Weight % U235	0.218
Oxygen-to-uranium ratio	2.01
Average particle size, in microns (Fisher sub-size method)	4.0
Particle density, g/cc (helium buoyancy method)	10.8 (98% theoretical)

The impurities are shown in Appendix B.

The samples were annealed at 1500°C, for a period of 6 hr, in a hydrogen furnace, to achieve a uniform uranium-to-oxygen ratio. After anneal, the powder was kept in a vacuum dessicator and was not exposed to air except for short intervals during transfers.

B. Infusion Stage

Figure 1 shows the schematics of the system used in the infusion stage. The details appear in Appendix A.

A tantalum crucible was filled with preannealed uranium dioxide and inserted in a high-pressure furnace designed for this purpose. The furnace was closed and left under high vacuum overnight. On the following day the furnace was flushed with helium three times, to minimize oxygen concentration. Each time helium pressure was allowed to reach nearly 1 atm, and then the furnace was evacuated. The vacuum line was closed and the furnace was pressurized at room temperature to a value that would result in the desired pressure at temperature T.

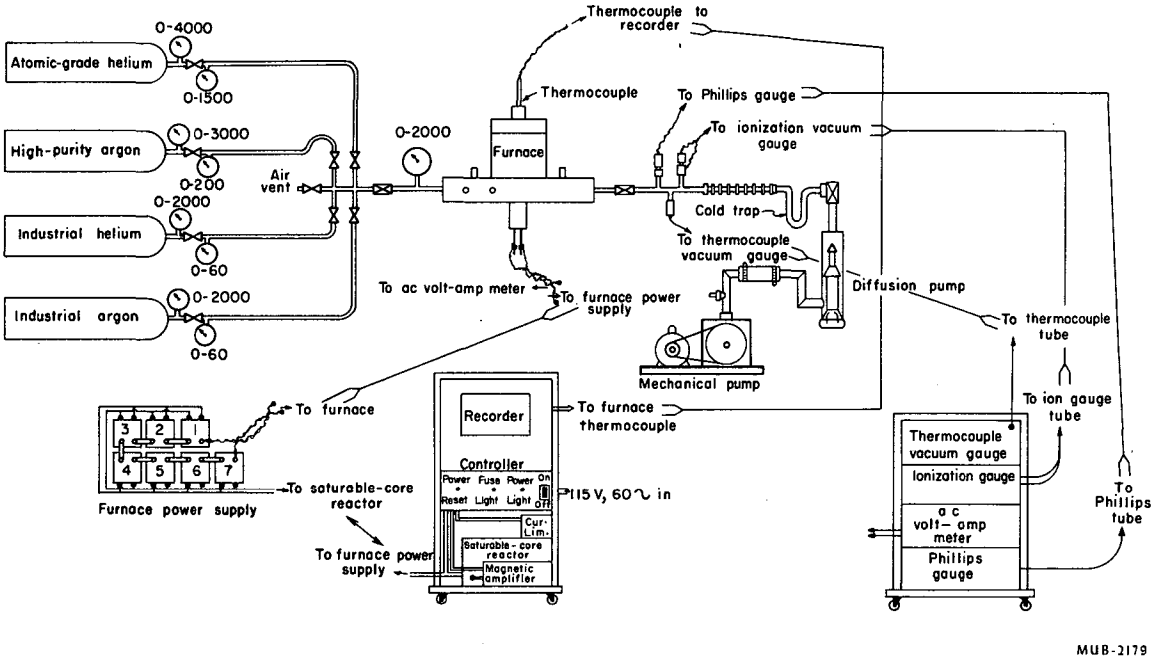

Fig. 1. Schematic arrangement of infusion system.

Leaving the temperature controller (described in Appendix A) on manual and minimum output, power was turned on and increased gradually until the final temperature was reached. This last step usually took about 15 minutes. Pressure was adjusted to the desired value, and the inlet line, controlled by a regulator, was left open to keep pressure constant. The regulator includes a safety valve that leaks at about 107 atm.

An ice bath was used for the thermocouple's cold junction. The recorder was checked for calibration before every run. The furnace could be left unattended except for periodic checkups, which were usually done once every 5 to 10 hr. Enough precautionary measures are taken to turn off the furnace in case of emergency.

At the end of every experiment the controller was set on manual, the inlet valve was closed, and power was decreased gradually and then finally turned off. This process took about 10 minutes. The furnace was allowed to reach to room temperature, and then pressure was released slowly to avoid scattering the sample out of the crucible. A tantalum lid covering the crucible prevents loss of the sample in case of accidental pressure release.

The furnace was opened then and the sample was transferred to a previously weighed, stainless steel crucible. The full crucible was reweighed accurately to determine the quantity of uranium dioxide, and was then kept under vacuum in a dessicator.

C. Isotope Dilution Stage

Samples were left under vacuum for about two months, before starting the isotope dilution stage. This process minimized the quantity of helium in open pores that might be present in the powder. Each crucible was then suspended in an induction chamber described in Appendix A. Vacuum pumps were turned on and trap 2 was immersed in liquid nitrogen to freeze mercury vapor (Fig. 2). Trap 1 was also filled to attain a better vacuum.

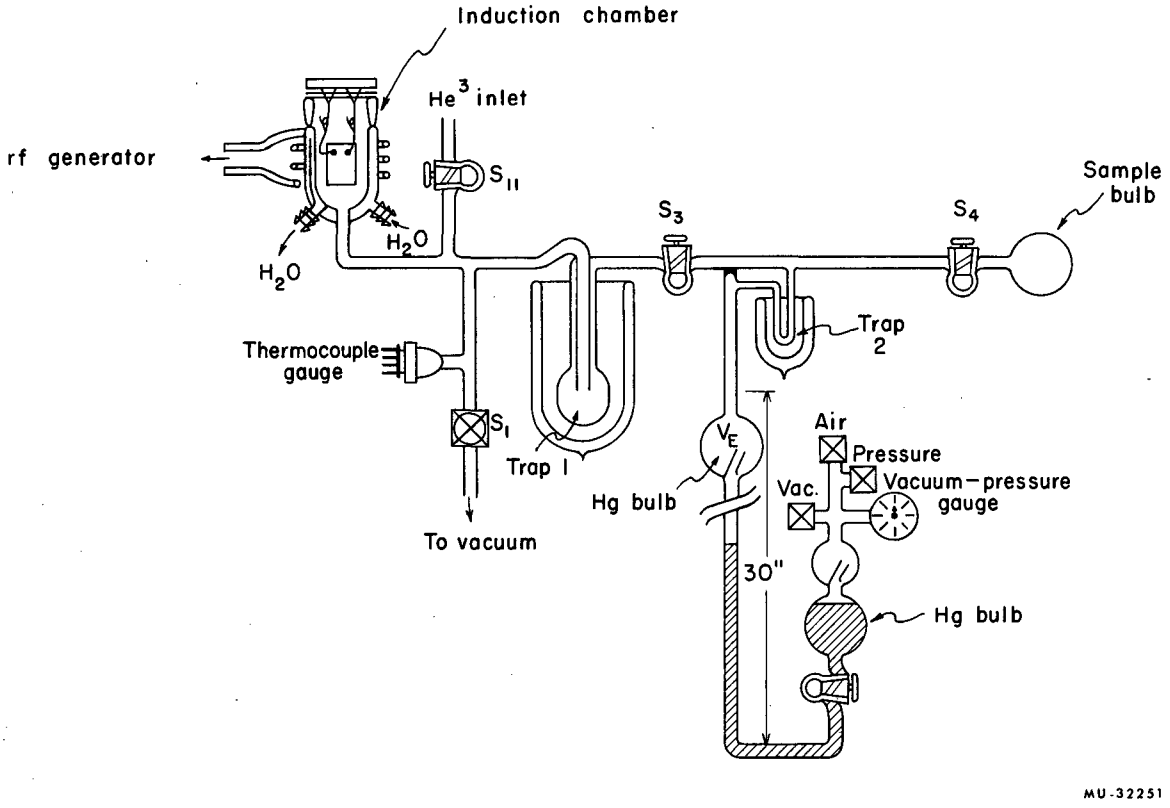

Fig. 2. Schematic arrangement of dissolution system.

When the ionization-gauge reading reached 10^{-4} torr, power to the induction coils was turned on. Pressure at the location of the ionization gauge usually increased to about 8×10^{-4} torr and decreased shortly after. Samples were annealed by this procedure at about 300°C for 3 hr to release the quantity of helium that might have been adsorbed on the surface of UO_2.

Power was turned off; thirty minutes later when the crucible had reached room temperature it was removed. A mixture of anhydrous sodium carbonate and potassium nitrate was added to the crucible. The crucible was suspended in the induction chamber again and was left under high vacuum overnight.

The next day, the He^3 delivery system (Fig. 3)–which had been under high vacuum, except for Chamber A–was prepared to deliver the desired quantity of He^3 (Appendix A). Monometer pressure was read by a cathotometer. The temperatures at V_D and the monometer were measured and recorded; they varied between 23 and 26°C. Stopcock S_{10} was then closed to trap the known quantity of He^3.

At this point value S_1 was turned off to close the isotope dilution system completely from vacuum (Fig. 2). Trap 1 was filled with liquid nitrogen and stopcock S_{11} was opened to release the measured quantity of He^3 into the dissolution system. Internal pressure of this system, as read by a thermocouple gauge, was less than 1 μ before introducing He^3. It was increased to 50-70 μ after the release.

One side of the Toepler pump was left at atmospheric pressure by leaving the air valve open. This would raise the mercury level approximately 15 cm above bulb E. Pressure of the system was monitored during the dissolving process by reading the mercury column's height.

While the sample was watched through the lid, the rf power was turned on and increased gradually until the sample started to dissolve. The beginning of the reaction is characterized by evolution of gases out of the mixture, similar to boiling.

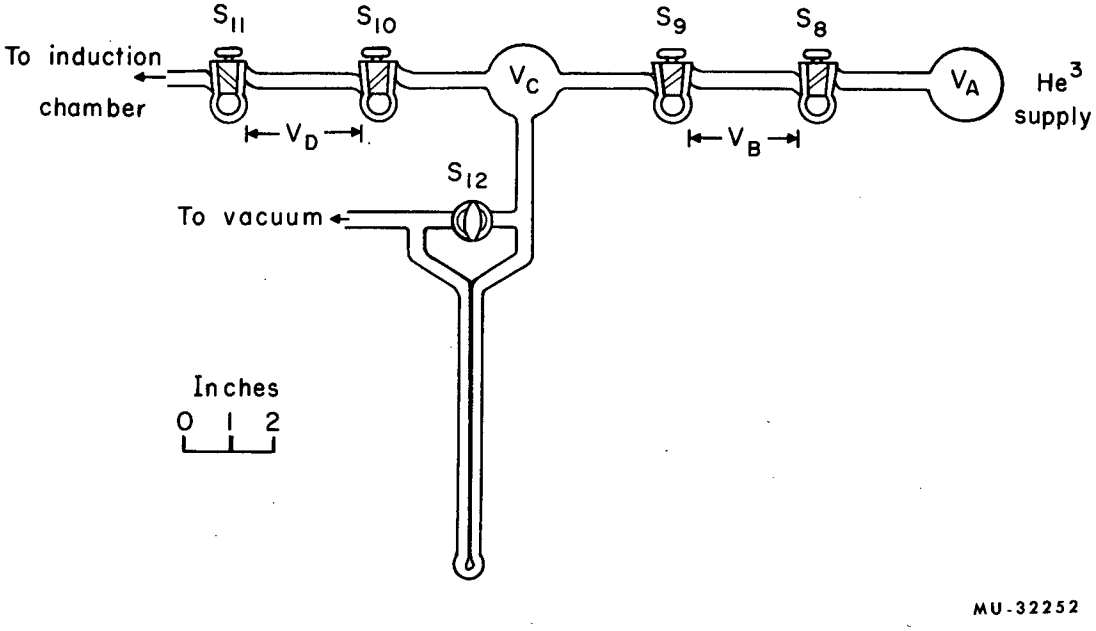

Fig. 3. Schematic arrangement of He^3 delivery system.

The samples occupied only half of the crucible's volume, to avoid loss of sample in case the reaction became violent. The temperature was finally raised to about 600°C. At the end of the reaction, indicated by a yellow-orange color, gases were collected in the sample bulb. This was done by lowering the mercury level to expand the gases into volume E. Then stopcock S_3 was closed to prevent gases from going back into the ionization chamber, and the mercury level was raised again to force the gases from volume E to the sample bulb. Then the sample bulb was closed off by stopcock S_4. Stopcock S_3 was opened and the mercury level lowered; this volume was forced into the sample bulb. This procedure was repeated twice.

To insure a uniform mixture of He^3 and He^4, the content of the sample bulb was released back to the ionization chamber and it was then recollected, by pumping 4 or 5 cycles.

The sample bulb was disconnected, labeled, and kept for mass spectrometric analysis. The system was cleaned, and the liquid-nitrogen bath of trap 1 was removed. The content of trap 1, mainly NO_2, was transferred to a glass bulb-immersed in liquid nitrogen-which connects to the system by tygon tubing, and was finally bubbled through water. Care was taken not to let NO_2 be in contact with Toepler-pump mercury for a long time since this would result in oxidation of mercury.

The system was left under vacuum after installing another sample bulb. The same procedure was followed for other runs. The He^3 delivery stage was simpler in those runs, since there was already He^3 at an acceptable pressure in volume C. The monometer pressure was read, however, to make sure that there had been no leakage of air into the bulb. A pressure increase of less than 1% was considered acceptable since it could be deducted from the monometer pressure to give the partial pressure of He^3.

IV. RESULTS

A. Data

Table I lists the conditions under which seven infusions were conducted. Pressure and time behavior were investigated at 1200°C, and a separate run was made at 1300°C. After the infusion stage the samples were dissolved to release He^4, a known quantity of He^3 was added, and the ratio of He^4 to He^3 was determined mass-spectrometrically. The results are shown in Table II.

B. Error Analysis

The data obtained at 1200°C (including that at 50 atm) are plotted against infusion time in Fig. 5. The estimated precision of the results are indicated by the vertical lines. The accuracy of the mass-spectrometric analysis was within about ± 1%. This was the main source of error in the experiment. The weights were measured with an accuracy within 1 part per thousand (ppt), and the pressure-reading inaccuracy was less than 6 ppt.

The quantity of He^3 added was measured within 6 ppt except for runs 1 and 2 where the assigned accuracy is within about 1%. This increase in inaccuracy is because of possible air leakage during the 24 hours that He^3 occupied the monometer volume. In the other runs fresh He^3 was used and pressure was checked periodically. The maximum leakage detected was less than ppt in 24 hr, which was subtracted from the total pressure. A leakage in such a case tends to cause an overestimate of the quantity of He^4 infused.

In Figs. 5 and 6 a precision within 1.5% is allowed for all the points, except for runs 1 and 2 where a precision within 2.5% is assigned.

Table I. Infusion conditions of samples.

Run	Temp. (°C)	P (atm)	Time (hr)	UO_2 weight (g)
1	1200	100	6.0	4.806
2	1200	100	8.9	4.506
3	1200	100	15.2	4.588
4	1200	100	46.9	3.026
5	1200	50	48.9	4.529
6	1200	100	71.4	5.031
7	1300	100	30.1	4.653

Table II. Experimental results.[a]

Run	He^3 added [cc (STP)]	He^4/He^3	He^4 dissolved in UO_2 (cc)	(cc/g)	cc/g-atm
1	3.04×10^{-2}	8.17	2.48×10^{-1}	5.16×10^{-2}	5.16×10^{-4}
2	2.99×10^{-2}	8.12	2.43×10^{-1}	5.39×10^{-2}	5.39×10^{-2}
3	3.08×10^{-2}	9.03	2.78×10^{-1}	6.06×10^{-2}	6.06×10^{-4}
4	6.63×10^{-2}	7.61	2.00×10^{-1}	6.61×10^{-2}	6.61×10^{-4}
5	3.16×10^{-2}	4.83	1.52×10^{-1}	3.36×10^{-2}	6.71×10^{-4}
6	2.72×10^{-2}	12.6	3.42×10^{-1}	6.80×10^{-2}	6.80×10^{-4}
7	1.38×10^{-2}	10.9	1.50×10^{-1}	3.23×10^{-2}	3.23×10^{-4}

[a]All cc at STP.

C. Validation of Henry's Law

Results of runs 2 and 5, performed under 100 and 50 atm external pressure, were used to investigate Henry's law for a He - UO_2 system (Fig. 4). The fact that the straight line, established by these two points, passes through the origin shows that Henry's law is obeyed accurately, and it also establishes dependability of the data. These two runs actually did not have exactly the same infusion time (Table I); but since a time difference of 2 hr close to saturation is not significant (as shown by a diffusion coefficient derived later), there was no correction made in Fig. 4.

D. Effect of Infusion Time

The values of helium solubility in UO_2, derived from runs 4, 5, and 6, are:

$$\bar{C}_5 = 6.61\times10^{-4} \quad \text{cc(STP)/g-atm},$$
$$\bar{C}_6 = 6.71\times10^{-4} \quad \text{cc(STP)/g-atm},$$
$$\bar{C}_7 = 6.80\times10^{-4} \quad \text{cc(STP)/g-atm}.$$

The difference between these values is of the order of the experimental precision, and hence they can be considered as representing the true solubility. If we take the quantity of infused helium at saturation to be 6.71×10^{-4} cc, the average of these three values, we can try to predict the data by using several values of diffusion coefficient in Eq. (8) and see if any of them correspond to experimental data at shorter times. Figure 20 shows the results as predicted by several diffusion coefficients. Considering Fig. 5, it is reasonable to assume that the solubility is not less than 6.71×10^{-4} cc. Hence the value of diffusion coefficient according to this data cannot be higher than 1.9 ± 10^{-13} cm^2/sec, since curve (a) in Fig. 5 is already quite far from the second and third data points. A higher diffusion coefficient produces a curve that will be even further from these points. This establishes an upper bound for diffusion coefficient equal to 1.9×10^{-13} cm^2/sec.

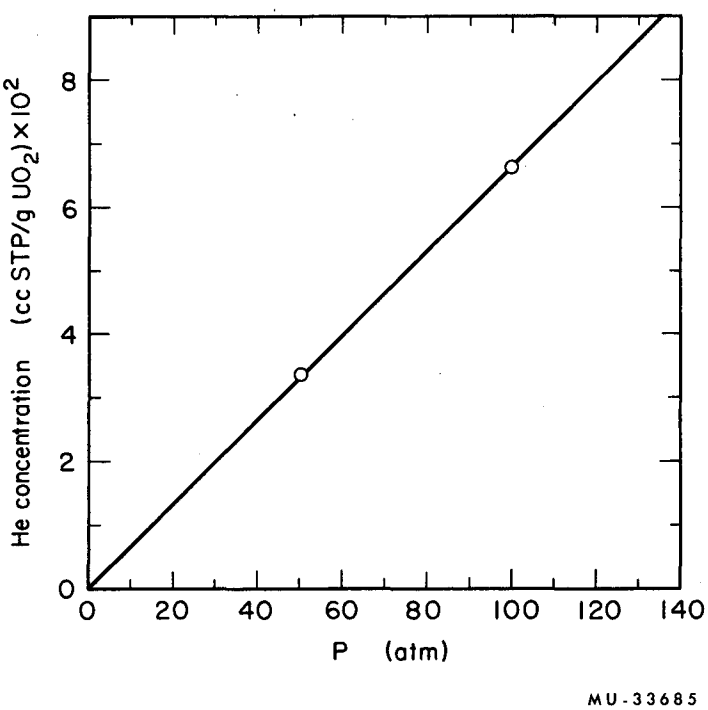

Fig. 4. Comparison of theoretical plot of Henry's law with experimental results for He-UO_2 system.

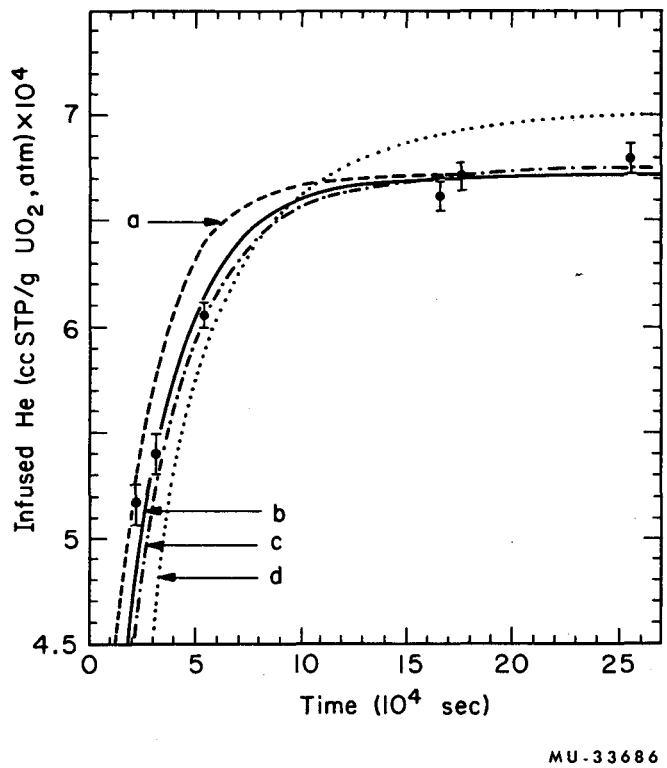

Fig. 5. Comparison of experimental results with theoretical curves.

a: $D = 1.9\times10^{-13}$ cm^2/sec, $C_s = 6.71\times10^{-4}$ cc,
b: $D = 1.5\times10^{-13}$ cm^2/sec, $C_s = 6.71\times10^{-4}$ cc,
c: $D = 1.3\times10^{-13}$ cm^2/sec, $C_s = 6.75\times10^{-4}$ cc,
d: $D = 1\ \times10^{-13}$ cm^2/sec, $C_s = 7\times10^{-4}$ cc.

To establish a lower bound, let $D = 1\times10^{-13}$ cm^2/sec. The best curve for this diffusion coefficient corresponds to a solubility of 7×10^{-4} cc. This curve is obviously too far from the data points.

As Fig. 5 shows, the value of diffusion coefficient is most likely in the range $(1.5\pm0.3)\times10^{-13}$ cm^2/sec. Figure 6 shows the theoretical curve corresponding to diffusion coefficient $D = 1.5\times10^{-13}$ cm^2/sec and solubility $C_s = 6.71\times10^{-4}$ cc.

E. Temperature Dependence

For a diffusion coefficient of 1.5×10^{-13} cm^2/sec, at 1200°C, 99% saturation is attained at about 30 hr. Since the diffusion coefficient obeys an equation of the form

$$D = D_0 \exp(-E/RT)$$

at 1300°C, it is expected to be higher than 1.5×10^{-13} cm^2/sec. It is hence reasonable to assume that the sample in run 7 had reached saturation.

The temperature behavior of solubility is given by:

$$\ln C_s = \frac{\Delta H}{R}\frac{1}{T} + \text{constant},$$

where ΔH is the enthalpy of dissolution and R is the gas constant. Using results of previous calculations for solubility at 1200°C, and run 7 for solubility at 1300°C, it is possible to get some idea about the enthalpy of dissolution for the $He-UO_2$ system.

According to Fig. 7,

$$\Delta H = 34 \text{ kcal/mole, } ^\circ K .$$

F. Comparison with Bostrum's Experiment

Reference 8 reports an experiment by Bostrum that dealt with infusion of helium in uranium dioxide. He used powder of 0.15-μ particle size in a pressure range of 1/2 to 2 atm at 600, 800, and 1000°C. The results of these experiments appear in Table III.

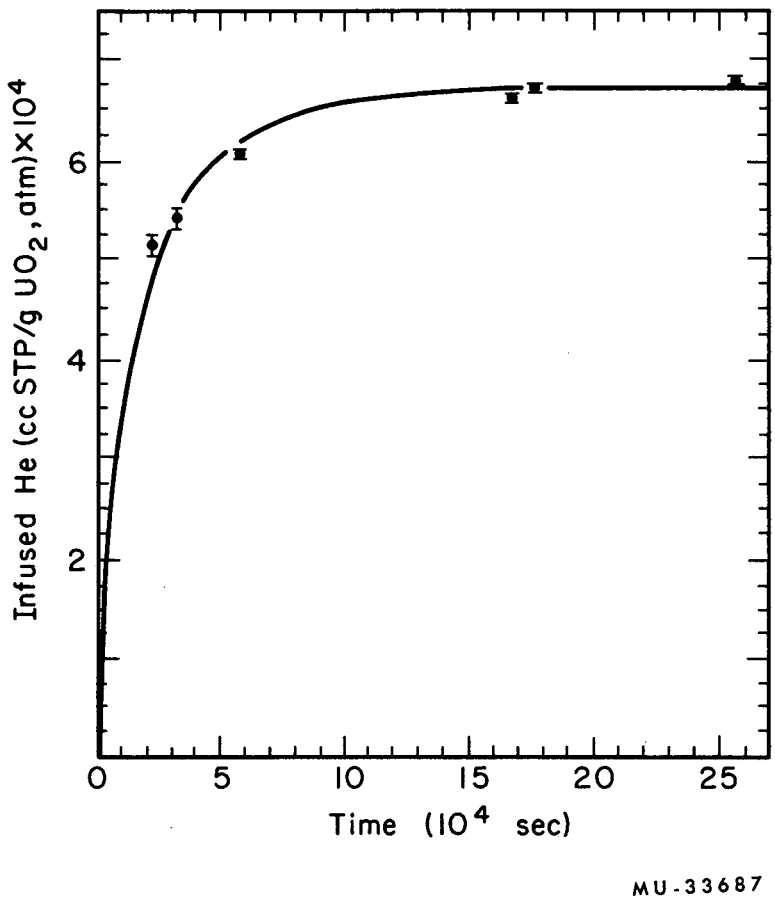

Fig. 6. Comparison of experimental results with theoretical curve[$D=1.5\times10^{-13}$ cm^2/sec, $C_s=6.71\times10^{-4}$ cc(STP)].

Table III. Data by Bostrom.

Temp. (°C)	Time (hr)	Pressure (atm)	He [cc (STP) $\times 10^4$]
800	4	1	1.2
800	8	1	2.3
800	16	1	2.4
800	24	1	2.4
800	36	1	2.5
800	64	1	2.3
800	16	1/2	0.45
800	64	1/2	0.79
1000	4	1	1.1
1000	8	1	1.1
1000	16	1	1.1
1000	40	1	1.1
600	48	1/2	0.18
	64	1	0.15
	48	2	0.52

The temperature behavior of solubility is plotted in Fig. 7. His data show a much weaker dependence of solubility on temperature than our data. Solubility of helium in uranium dioxide at 1200°C, as predicted by Bostrom's data, is about 7×10^{-5} as compared to 6.71×10^{-4} cc/g-atm based on the data in our experiment—or one order of magnitude higher.

The dependence of infused helium on pressure, as derived from Bostrom's data, is shown in Fig. 8, for comparison with Fig. 4.

It is difficult to correlate Bostrom's data with Henry's law and our work. In view of the precision attained in our work, it is concluded that the He-UO_2 system does obey Henry's law.

G. Conclusions

The solubility of helium in uranium dioxide at 1200°C was measured to be $6.71\times10^{-4}\pm 1.5\%$ cc(STP) per gram of UO_2 per atmosphere of helium pressure. Solubility at 1300°C was 3.23×10^{-4} cc(STP)/g UO_2-atm. The accuracy is expected to be within about 2% based on the runs at 1200°C.

It was shown that the He-UO_2 system obeys Henry's law. The value of the diffusion coefficient as derived from the time plot at 1200°C is $(1.5\pm0.3)\times10^{-13}$ cm^2/sec. An approximate value for the enthalpy of dissolution for the He-UO_2 system was determined from a semilogarithmic plot of solubility vs inverse of temperature. This value was about 34 kcal/mole, °K.

Three runs were made at 1500 and 1800°C. Since the diffusion coefficient was underestimated, infusion time was set too high, which resulted in sintering of samples. Infusion time at 1500°C was 6.16 and 48.5 hr; at 1800°C the time was 2.34 hr. The mass-spectrometric analysis of these runs showed apparent solubilities that were too high to be realistic and the data was inconsistent. The discrepancy was attributed to inclusion of helium between powder particles during sintering. It is recommended to try short infusion time runs in the temperature range 1300 to 2000°C.

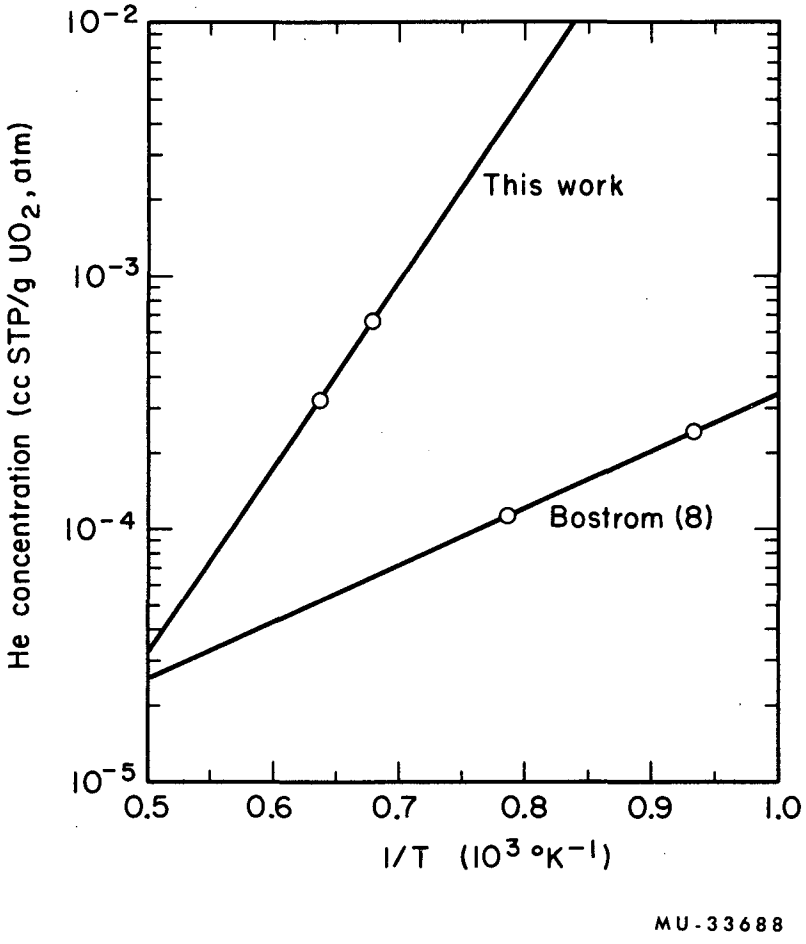

Fig. 7. He solubility vs temperature.

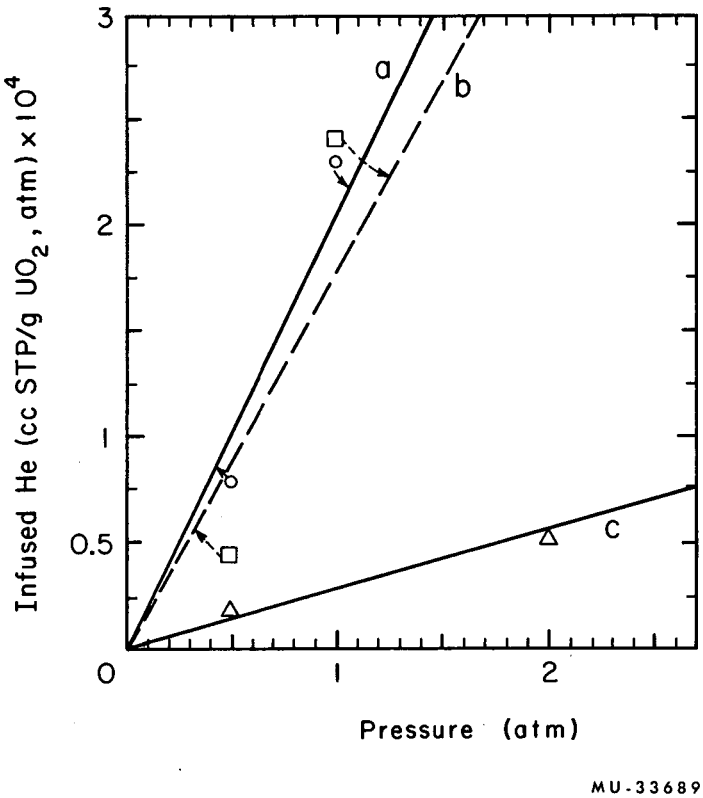

Fig. 8. Comparison of Bostrum's data with Henry's law.

a: T = 800°C, t = 64 hr, ,

b: T = 800°C, t = 16 hr, ,

c: T = 600°C, t = 48 hr, .

Investigation by this method of the solubility and diffusion coefficient of other gases, especially Xe and Kr, is also recommended since the equipment needs minor changes to be able to handle those experiments. The only change required is to replace the He^3 supply bulb by some gas similar to the one used for infusion.

The isotope dilution apparatus can be improved by:

(a) Enlarging the volume of the Toepler pump (Fig. 13), by using a 300-cc bulb for V_E to facilitate pumping.

(b) Delivering larger quantities of He^3 to match the expected value of He^4; i.e., to give $r = He^4/He^3 \approx 1$. This can be done using a higher-pressure supply bulb, and mercury in the monometer rather than oil.

ACKNOWLEDGMENTS

The author would like to express his gratitude to:

Professor Thomas H. Pigford who initiated and supervised this research, and gave guidance that led to the results.

Dr. Donald R. Olander for his valuable advice on problems as they arose for his interest in this work.

Dr. Richard M. Fulrath for many helpful meetings.

Mr. Marshall Williams for his help on the apparatus.

This work was done under the auspices of the U. S. Atomic Energy Commission.

APPENDIXES

A. Apparatus

1. Infusion System

a. Furnace design. A high-temperature furnace was designed and constructed which could be operated at 2000°C in the pressure range 100 atm to 10^{-5} torr. Figure 9 shows a cross section of the furnace. The heating element is 0.001-in.-thick tungsten ribbon, 5-3/4 in. long and 1/2 in. wide, which was cut from a sheet by a pair of scissors. The ends of the ribbon are cut wider than the middle to keep the temperature at the ends low (Fig. 11a). Three slots are made at each end to allow the heating element to be attached to electrodes which essentially are two quarters of a hollow cylinder, as seen in Fig. 10. The upper half is tantalum and the lower section of each electrode is made from stainless steel and is brazed to the tantalum section. Two tantalum plates are fastened to each electrode by three screws. Each end of the heating element is put between the plates and is tightened by the screws to make good electrical contact. A small tantalum weight rides on the heating element to keep it from buckling. Two 8-gauge stainless steel rods, welded to the base of the electrodes, carry electrical current to the furnace. The welded joints rest on a piece of mica which in turn sits on the base-plate of the furnace.

Three sets of radiation shields surround the heating element. One set is made from a 0.001-in.-thick tungsten sheet 2.5 in. wide and approximately 25 in. long. The sheet is rolled into an eight- to nine-turn tube and slips into a tantalum cylinder to keep a 1-1/4 in. o.d. The tantalum cylinder is made from a 0.005-in.-thick sheet that is spot welded at the ends. If fits snugly between the two electrodes and is electrically insulated from them by a thin sheet of mica (Fig. 9). To minimize conduction of heat radially, the radiation shields are dimpled randomly such that the layers make contact only at the dimpled spots.

A 1-5/8-in.-o.d. and 5/8-in.-i.d. ring (Fig. 11c) made from 0.01-in.-thick tantalum is placed on the electrodes (Fig. 9) and is

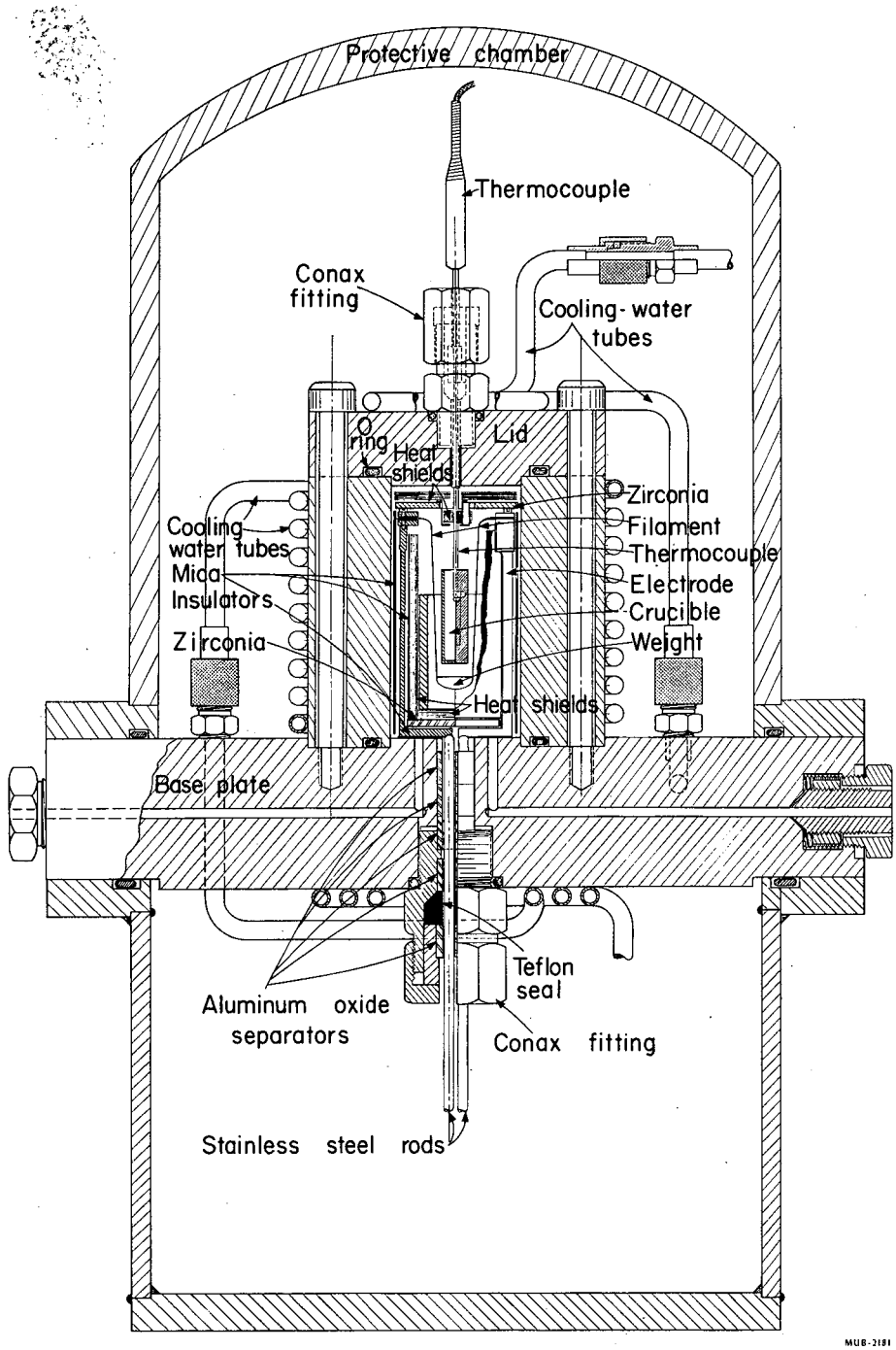

Fig. 9. Cutaway view of furnace.

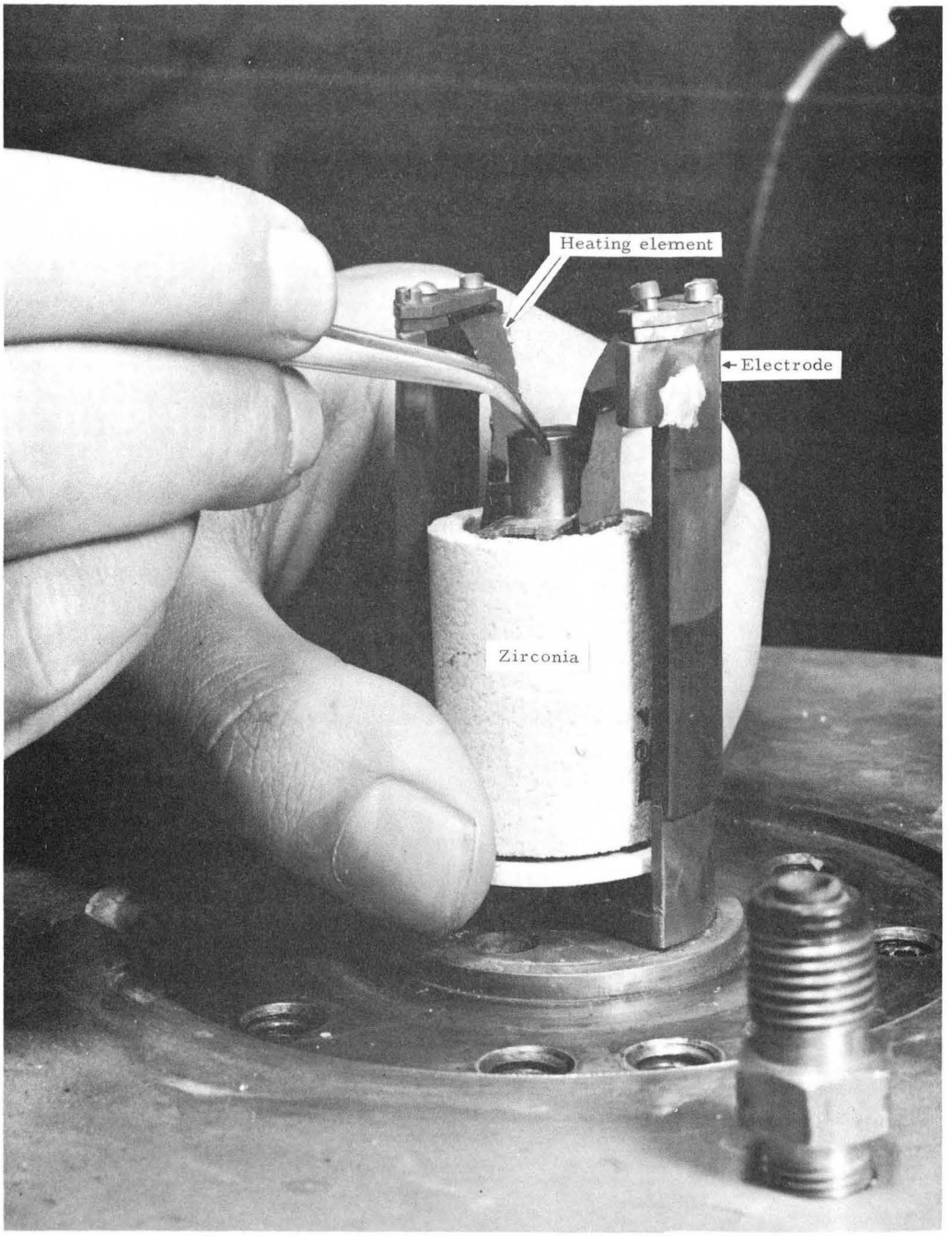

ZN-4028

Fig. 10. Furnace heating assembly.

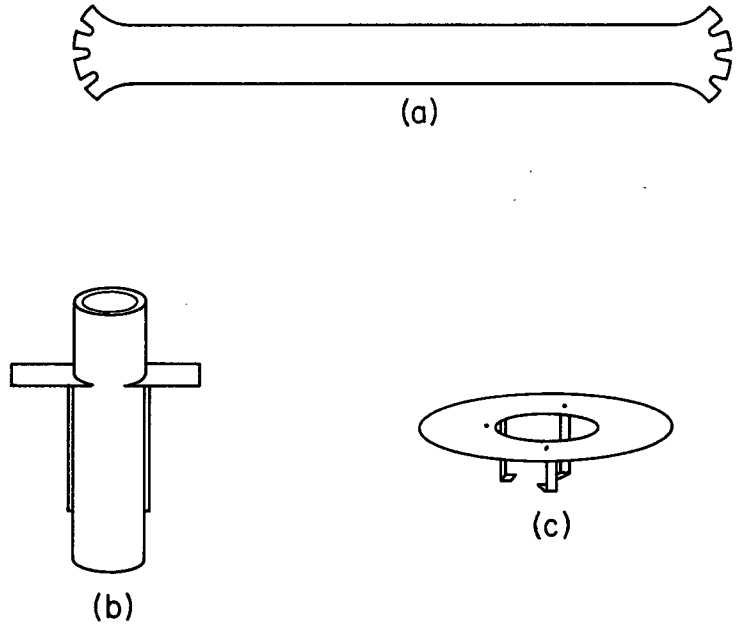

MU-33690

Fig. 11. Sketches of (a) heating element, (b) tantalum crucible, (c) tantalum ring.

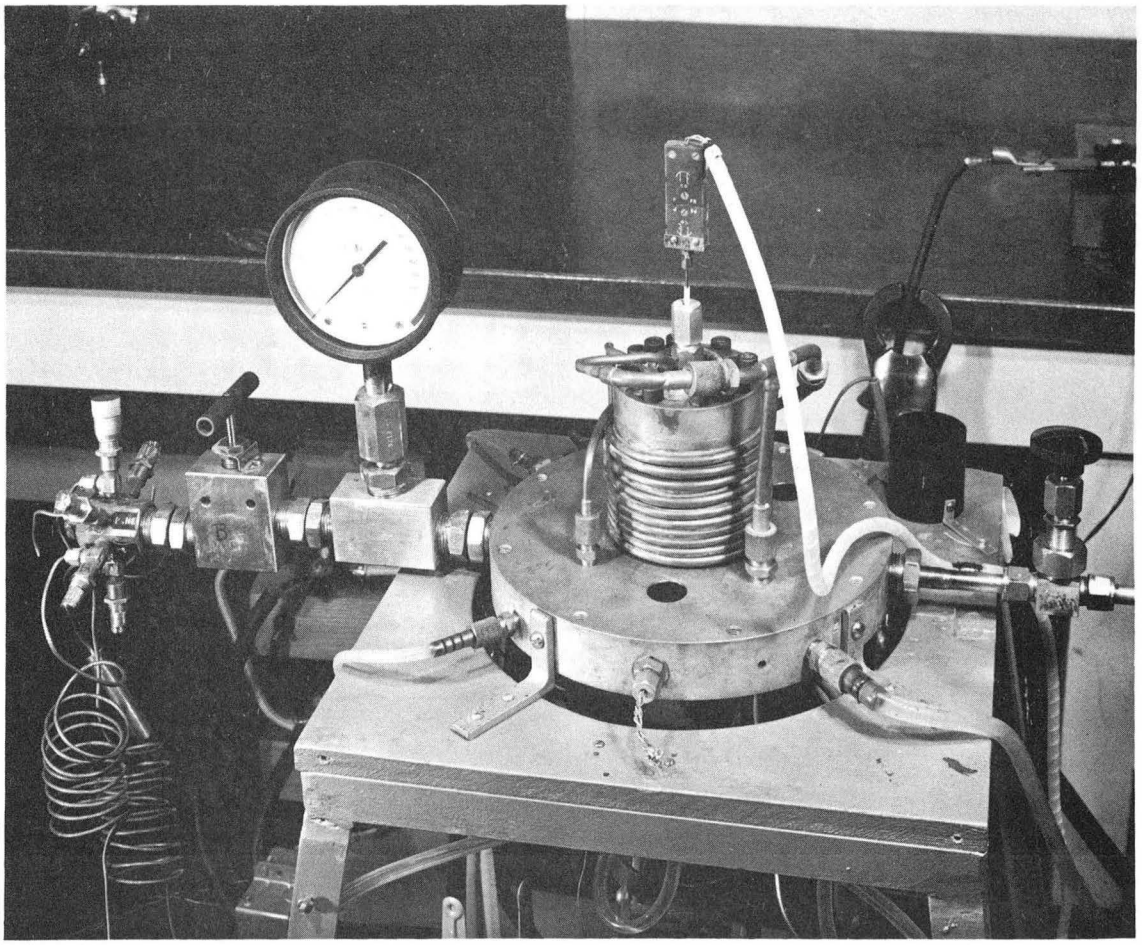

ZN-4027

Fig. 12. Over-all view of furnace.

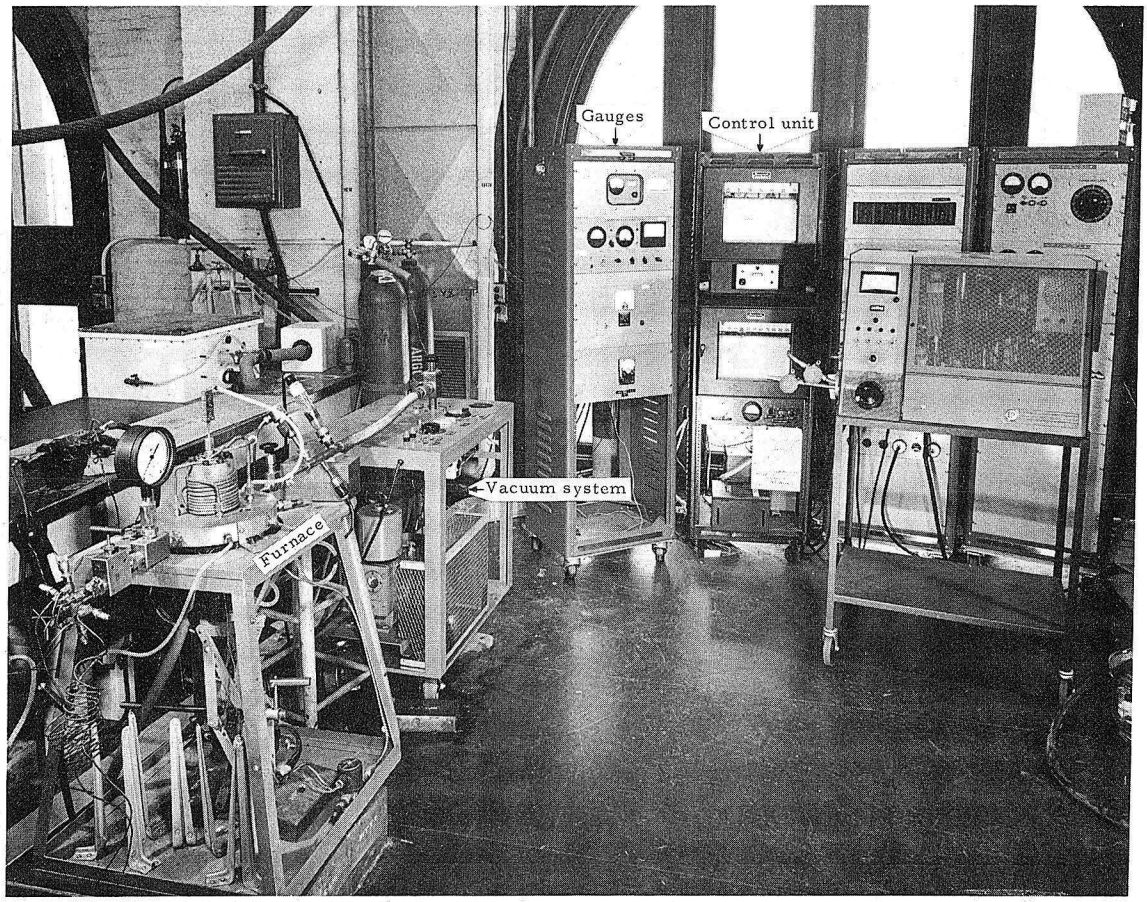

ZN-4026

Fig. 13. Complete infusion system.

electrically separated from them by a 1/16-in. zirconium oxide ring. Three legs are spot-welded to the ring to support a set of 1/2-in.-diameter radiation shields which reduce absorption of heat by the electrodes. Eight 1-5/8-in.-diameter shields are placed on top of the ring. Each one has a 1/8-in. hole in the center to allow a thermocouple to pass through.

Finally, a set of eight 1-in.-diameter disks minimize heat flow to the base-plate of the furnace. A 1/16-in.-thick zirconium oxide disk separates them from the electrodes (Fig. 9).

The sample crucible (Fig. 11b) is a 1-1/4 in.-long cylinder having a diameter of 3/8 in. It is made by boring a tantalum rod to 0.03-in. wall thickness. With powdered samples, a lid with a 1/8-in. hole at its center covers the top. (If pressure inside the furnace is suddenly released, the powder will tend to spew out.) Tantalum rods are heliarc-welded to the crucible by two brackets. To support the crucible, a 1-in.-o.d. zirconium oxide cylinder having a wall thickness of 1/8 in. is slipped inside the radiation-shield tube. The crucible rests on this cylinder by its arms. The ZrO_2 cylinder also provides electrical insulation between the heating element and the radiation shields.

Because of its high thermal conductivity and ease of machining, the pressure shell is made from brass. Thin sheets of mica electrically insulate the pressure shell from the electrodes. The pressure shell has an effective wall thickness of 1/2 in. and is separable from the base-plate to allow free access to the electrodes. Two 3/8-in. Allen-head steel bolts hold the pressure shell to the base-plates. A 1/8-in.-deep by 1-1/8-in.-wide groove is cut in the base plate to center the pressure shell (Fig. 9). A 1/8-in.-deep by 1/8-in.-wide O-ring groove in the bottom of the pressure shell takes a 1/8-in. neoprene O ring to seal it to the base plate.

The lid is a 7/8-in.-thick brass disk having a diameter of 4 in.; it is attached to the pressure shell by two 3/8-in. bolts. Finally, eight similar bolts secure the lid to the base-plate after passing through the wall of the pressure shell. The central portion of the lid is raised

1/8 in. to fit snugly inside the pressure shell for centering. An O ring groove similar to that of the pressure shell accommodates a 1/8-in.-thick neoprene O ring (Fig. 9).

The inlet line is connected to a USG, 0-2000-psi pressure gauge and a Whitey High Pressure Valve by high-pressure, union-type fittings. Six different gas lines can be brought into the system by 1/8-in. copper tubing; each one of these is controlled by a Nupro high-pressure needle valve.* These valves are mounted on a hexagonal stainless steel block to minimize the gas volume. One of these valves is provided with a micrometer head in case a carrier gas flow is desired. The gas will pass through a gas flow meter incorporated in the line.

A 1/4-in.-i.d. vacuum line, provided 180 degrees from the inlet, passes through the base-plate and ends to a high-pressure valve similar to that on the inlet line.

The two 8-gauge rods attached to the electrodes are brought out of the furnace through the base-plate by a Conax gland, the cross section of which can be seen in Fig. 9. The rods are centered by aluminum oxide separators and pass through a seal that is compressed by a metal sleeve. Neoprene, Teflon, or lava can be used as sealant. Although a vacuum-tight seal can be most easily achieved with neoprene, and lava has the best high-temperature characteristics, Teflon proved to be the most appropriate sealant for this case since it is a compromise between the two.

A third hole can be drilled through the sealant and the aluminum oxide separators to insert an auxiliary thermocouple in addition to the main thermocouple, which is inserted through the lid of the furnace by a similar Conax fitting. Neoprene is used as a sealant since the temperature in this region is low. The thermocouple wires are of tungsten and rhenium insulated by beryllium oxide, covered by a 1/16-in. diameter tantalum sheath.

The temperature as read by the top thermocouple is more dependable since its hot junction is actually imbedded in the sample.

---

*American Instrument Company, Super Pressure Fittings.

The bottom thermocouple can only detect the temperature of the heating element's lower surface.

Copper coils cover most of the surface of the pressure chamber and connect to the water inlet and outlet provided through the base-plate. A stainless steel protective chamber covers the furance (Fig. 9) and makes a vacuum-tight seal with the base-plate. A thermocouple gauge monitors vacuum inside the chamber, which can also be filled with an inert gas if necessary.

To prolong the life of the sealant, it is advisable to cool the stainless steel rods, which carry current. When the protective shell is not used, the simplest method of cooling is to immerse the leads in a water-filled glass jar provided with an inlet and outlet that connect to the main cooling coil of the furnace. The glass jar rests on a jack which would ordinarily be used to raise the lower half of the protective chamber to the base-plate. A solenoid valve shuts off the water supply in case a leak develops in the furnace. When the protective chamber is in use the leads are in contact with water-cooled copper blocks.

The vacuum system consists of an oil diffusion pump backed up by a mechanical pump. A liquid-nitrogen trap is placed before the vacuum line and is connected to the furnace valve by copper bellows to eliminate vibration (Fig. 1). Vacuum gauges are located immediately before the Whitey valve. Thermocouple and ionization gauges allow continuous reading from 5×10^{-1} to 10^{-7} torr, and a Philips gauge is used for reference.

b. Control unit. Temperature is measured by a tungsten-rhenium thermocouple when operating in the range 1300 to 2000°C. For lower temperatures, chromel-alumel thermocouples are used. The millivolt output of the thermocouple is read and recorded on a Honeywell Electronic Stripchart Recorder, which uses a potentiometer measuring circuit and has a 0-40 mV input. However, when in use with a chromel-alumel thermocouple, the range is changed to 0-50 mV by changing a slide wire and a set of resistors.

The thermocouple supplies signal to a Honeywell Three-Mode Electrovolt control unit whose action is initiated by a deviation signal which is developed across a proportioning resistor, an integral part of the control unit. The deviation signal is fed to the control unit where it is acted upon by a proportional and rate action which results in a dc control current for a magnetic amplifier. The unit includes a reset action which continuously readjusts the current output of the control unit. The magnetic amplifier operates a 3-kW saturable core reactor.

A set of eight 5-V output transformers (Fig. 14) are used in series to step down the voltage. Each transformer accepts either 110 or 220 V on the primary and is rated for 115 A on the secondary winding.

The current delivered to the furnace is controlled by a Honeywell Automatic Current Limiter (Fig. 14). If the load current exceeds a prescribed value, the current limiter sends a signal to the magnetic amplifier that partially overides the "full heat" signal from the controller. This reduces the magnetic amplifier's output which in turn raises the impedence of the saturable reactor and causes less current to flow.

c. Safety circuits. Several safety mechanisms are incorporated in the system so that the furnace can be left unattended when in operation.

One circuit is designed to prevent use of the furnace without cooling water. In case of water failure, power to the furnace is automatically shut off and stays off until a reset button is activated. If water flow is resumed, it is important to keep power off until temperature and pressure controls are set on manual since resumption of operation in such a case might cause temperature and pressure to exceed the set point of the run.

The circuit consists of a flow-sensing microswitch which turns on at a flow rate of 1 gpm and off at 0.5 gpm (Fig. 14). The flow switch is connected in series with the coil and armature of an ac relay, which is in parallel with a normally open reset button. The coil of a high-current contact, single-pole relay is in series with the armature and

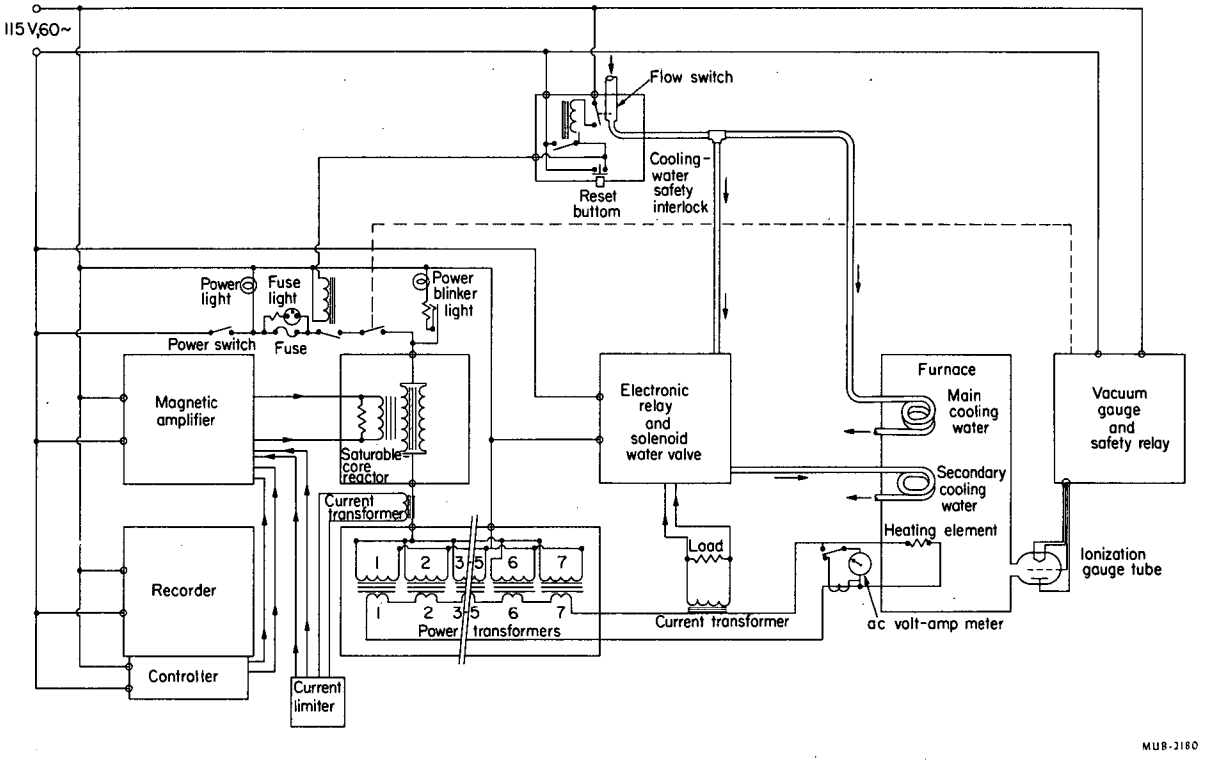

Fig. 14. Electrical schematic of infusion system.

reset button. This series arrangement is across the ac line. The single-pole relay is normally open and its armature is in series with one side of the power line to the furnace power transformers. When water flow is sufficient, pushing of the reset button will cause the relay to pull in and lock in the "on" position, activating the power relay which in turn allows power to be applied to the furnace. If water flow goes below minimum the microswitch opens and the coil releases the armature.

In vacuum operations, a serious leakage during a run can destroy the sample and the thermocouples if power is not turned off. Pressure is continuously monitored by an ionization tube vacuum gauge during a run. A relay is incorporated in the vacuum-gauge power supply, which is activated whenever the pressure exceeds a preset point. This in turn activates the relay in series with the power line and therefore turns off the furnace and the diffusion pump, and activates an alarm. Maximum tolerable pressure can be set anywhere from 10^{-6} to 10^{-2} torr. A bypass switch eliminates this circuit when necessary.

Water supply to the electrode-cooling jar can be cut off by an auxiliary circuit in case of leakage or any form of power failure even if an open circuit is developed. The system includes a solenoid valve that is open only when current flows through the furnace. A current transformer with a ratio of 1:50 is used in series with the furnace power transformers. The current transformer delivers 3 V across a 1.5-Ω load. When this voltage is rectified and applied to the grid of a triode, a relay in the plate circuit is tripped that activates the solenoid valve, allowing water to flow in the cooling bath. The flow rate is varied by a manual valve in series with the solenoid valve. The relay is connected in the circuit in a nonlocking manner so that water flow stops whenever there is no current passing through the furnace.

d. Operation. Since the furnace is well protected by radiation shields, the amount of heat loss is quite low. Power input required to reach 2000°C at 100 atm of pressure does not exceed 2 kW, at less than 80 A. This feature of the furnace eliminates various problems that

arise in other furnaces because of higher current requirements. In most designs, four water-cooled tubes must be brought into the furnace. This could not be tolerated since it would require a large volume. In this case two 8-gauge stainless steel rods (0.160-in. o. d.) carry the current into the chamber.

Heat losses were much lower in vacuum operation. The power input required to reach 2000°C in vacuum is about 800 W at about 50 A.

Figure 15 shows variation of temperature with power in a typical run. Power was turned on with an internal pressure of 64 atm. The final pressure at 2000°C was adjusted to 100 atm. In a different run the initial pressure was chosen to be 36 atm. Heat loss at 2000°C and the final pressure of 50 atm was 1600 W (Fig. 16). A vacuum run is demonstrated in Fig. 17.

By comparing the results of Figs. 15, 16 and 17, it is clear that an increase in pressure from vacuum to about 50 atm increases heat loss appreciably. However, further increase in pressure does not change power requirements to a great extent.

The effect of pressure on power is eliminated in Fig. 18. It represents variation of temperature with power at a constant pressure of 50 atm. Figure 19 shows dependence of pressure on central temperature in the particular temperature gradient of the furnace.

One of the characteristics of this furnace is its fast response, which makes temperature control simple. The temperature has been maintained practically constant for periods as long as 4 days, with the limits of accuracy being set by the recorder and the thermocouples. Because of its fast response, the temperature was controlled mainly by the proportional action of the Electro Volt Controller, using very little time or reset action.

Another feature of this furnace is its high endurance to thermal shock. No problems arise from expansion and contraction of the parts that are located in the high-temperature zone, since all of these parts are free from constraint. The ceramic parts would seem to be the weakest element of the system for thermal shock; however, this problem

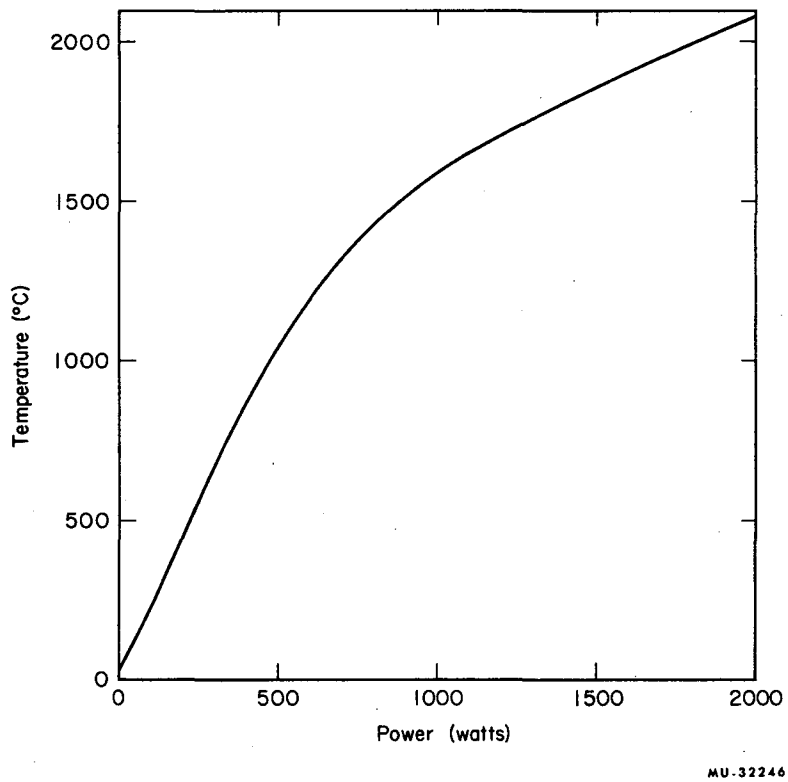

Fig. 15. Variation of furnace temperature with power input for 64-atm starting pressure.

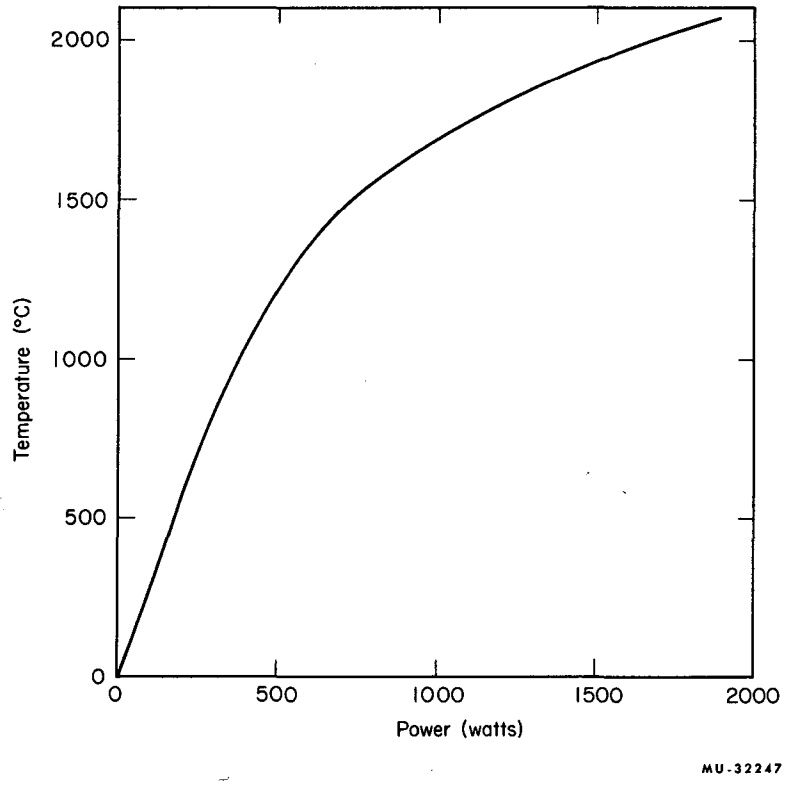

Fig. 16. Variation of furnace temperature with power input for 36-atm starting pressure.

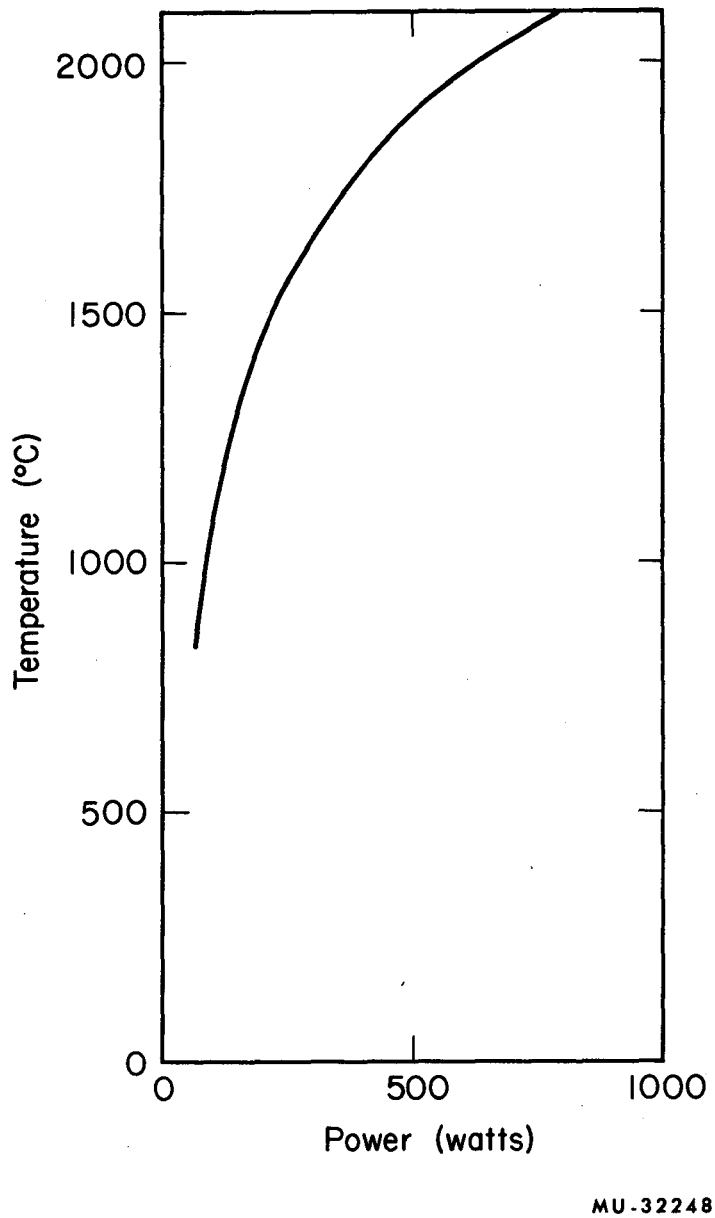

Fig. 17. Variation of furnace temperature with power input at vacuum.

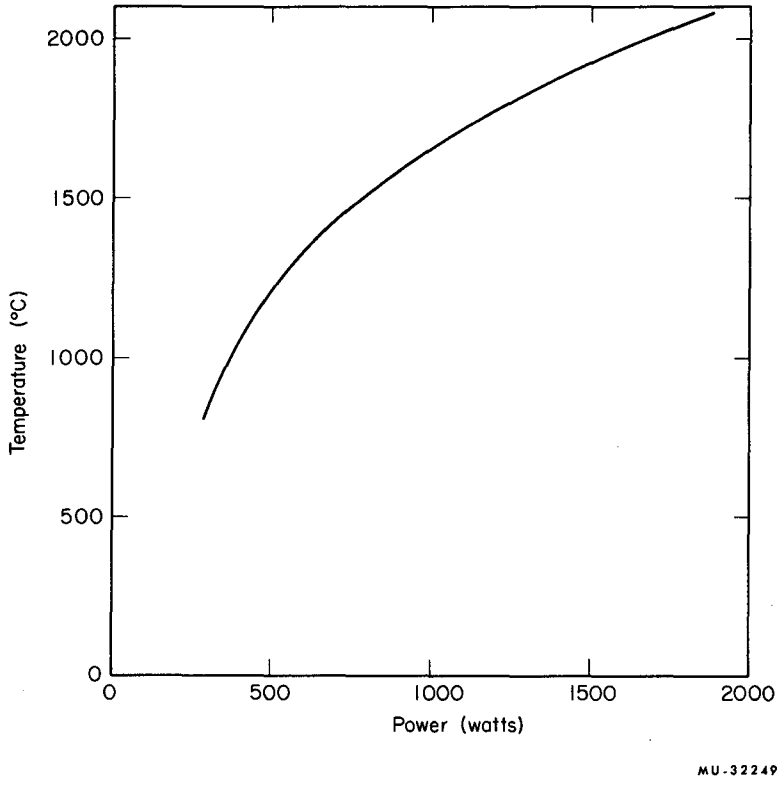

Fig. 18. Variation of furnace temperature with power input at a constant pressure of 50 atm.

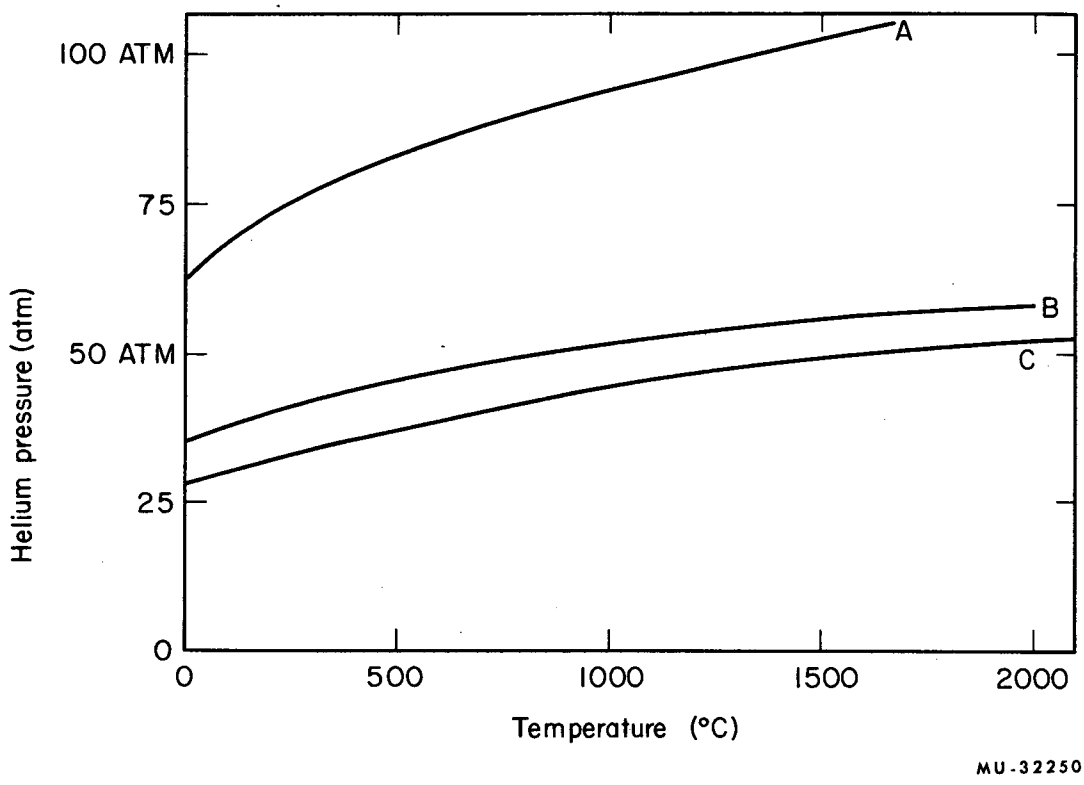

Fig. 19. Variation of pressure with central temperature of furnace.

was solved by using coarse-grain zirconium oxide.

Fine-grain zirconium oxide can be machined quite accurately, but it does not withstand thermal shock. The ceramic cylinder that supports the sample holder is coarse-grain zirconium oxide, made from commercially available crucibles. It is cut to the desired lengths and its wall thickness is reduced slightly to fit inside the radiation-shield tube. The cylinder has gone through many sharp thermal cycles and has proved to be quite dependable.

All the other ceramic parts are made from fine-grain zirconium oxide since they are not located at hot spots. The zirconium oxide ring that provides electrical insulation between the top radiation shield and the electrodes occasionally breaks in half; the two half rings can still be used as insulation, since no further cracking occurs.

Some of the surfaces were coated with zirconium oxide, using a plasmatron for electrical insulation. This did not prove to be successful since the layers of zirconium oxide flaked off upon heating.

The furnace can be brought to full temperature in 5 to 10 min. At one time the furnace experienced for 4 hr an oscillation at 1000°C with an amplitude of about 500°C and a period of 1 min. The furnace was able to tolerate this oscillation without developing any mechanical difficulties. (This situation occurred because a high reset action was used in the automatic temperature control; reset rate was decreased and the operation was continued normally.)

This system has been used for as long as 100 hr at one time. Longer runs are possible but have not been tried.

It is important to keep the system at a low oxygen content while at high temperature. The most susceptible part to oxidation is the thermocouple. When adequate care was taken, W/Re thermocouples had a life time of about 1000 hr. These W/Re thermocouples are covered in a thin tantalum sheath. Oxidation of this surface creates a leakage and therefore burns up the hot junction. This is not a serious problem when chromel-alumel thermocouples are in use.

The tungsten filament becomes rather brittle if exposed to oxygen at high temperatures. The average life of the filament has been

about 500 hr. In most experiments it is important to keep the furnace free of oxygen to prevent oxidation of the sample.

One method to increase the lifetime of the thermocouples and the heating element is to make some of the radiation shields from 0.001-in.-thick zirconium. Since zirconium is a better reducing agent than tungsten or tantalum, most of the oxygen will be reached by it. Usually the second radiation shield was chosen for this purpose, since it has the appropriate temperature for oxidation. Leakage of oxygen into the furnace can be minimized by evacuating the volume between the pressure shell and the protective chamber, or by filling it with an inert gas.

Pressure is kept constant by a high-pressure delivery regulator which can deliver up to 1500 psi. The quantity of gas leaked out of the furnace will be supplied by the regulator. By this method it is possible to keep the pressure constant at 100 atm, with less than 2 ppt, at 2000°C, for a period of 4 days. The most successful technique for detecting leaks was to pressurize the system to 100 atm of He and use a leak detector provided with a sniffer probe.

2. Isotope Dilution System

a. Dissolving of samples. Uranium dioxide samples are dissolved in a mixture of sodium carbonate and potassium nitrate heated in an induction furnace. The apparatus consists of an induction chamber which has a flat, clear lid to allow observation of the dissolution process (Fig. 2). Three hooks allow a stainless steel crucible to be suspended in the center of the chamber by three stainless steel wires. The chamber's volume has been minimized to simplify collection of helium in the sample bulb. The sample bulb has a volume of 50 cc, as compared to approximately 200 cc total value. A water-cooled jacket is provided on the chamber since its walls are only 1/4 in. from the crucible. Induction coils are situated outside the chamber, adjacent to its water jacket.

A Toepler pump is incorporated in the system to mix and collect gases in the sample bulb. It is operated by vacuum, air, and pressure lines, each controlled by a vee-stem Hoke valve. A vacuum and

pressure gauge predicts the behavior of mercury level before it is operated.

Gases evolved during the dissolution process pass through two traps before entering the sample bulb. The first trap eliminates extraneous gases such as NO_2 and CO_2 produced from dissociation of carbonate and nitrate flux; the second one prevents mercury vapor from entering the sample bulb. Mercury hammering is prevented by curved inlets in mercury bulbs.

A thermocouple gauge monitors internal pressure when the system is closed from vacuum.

b. Helium-3 delivery. This system is designed to deliver any desired quantity of He^3 in the range 10^{-3} to 2×10^{-1} cc (STP) in one operation. In principle, this method uses successive expansion of minute quantities of He^3.

The schematics of this system are shown in Fig. 3. Volume A contains 50 cc of He^3 at a pressure of 180 torr. Measurement of the gas quantity depends on an approximate knowledge of the volumes B and C, and an accurate knowledge of volume D, trapped between stopcocks S_8 and S_9. These volumes are determined before assembly; $V_B = 2.2$ cc, $V_C = 97$ cc, and $V_D = 2.285 \pm 1$ ppt. The complete system up to stopcock S_8 is evacuated thoroughly. Then S_9 is closed and S_8 is opened to allow He^3 to occupy volume V_B at a pressure of about 180 torr. Then stopcocks S_8, S_{11}, and S_{12} are closed and the amount of gas contained in V_B is allowed to expand to a total volume of $(V_B + V_C + V_D)$, by opening S_9. Pressure is read accurately by an oil monameter about 20 cm long. A cathetometer allows an accuracy of 2 ppt in pressure readings at 10 cm oil. Knowing volume, pressure, and temperature of V_D, the quantity of gas trapped between the two valves can be determined within a few parts per thousand. This quantity can be varied as desired by releasing or introducing more He^3 into the system.

An oil diffusion pump and a mechanical pump make up the vacuum system (Figs. 20-23). Pressure is read by thermocouple and ionization gauges. At higher pressures, during dissolution, the mercury column of the Toepler pump is used to determine the pressure.

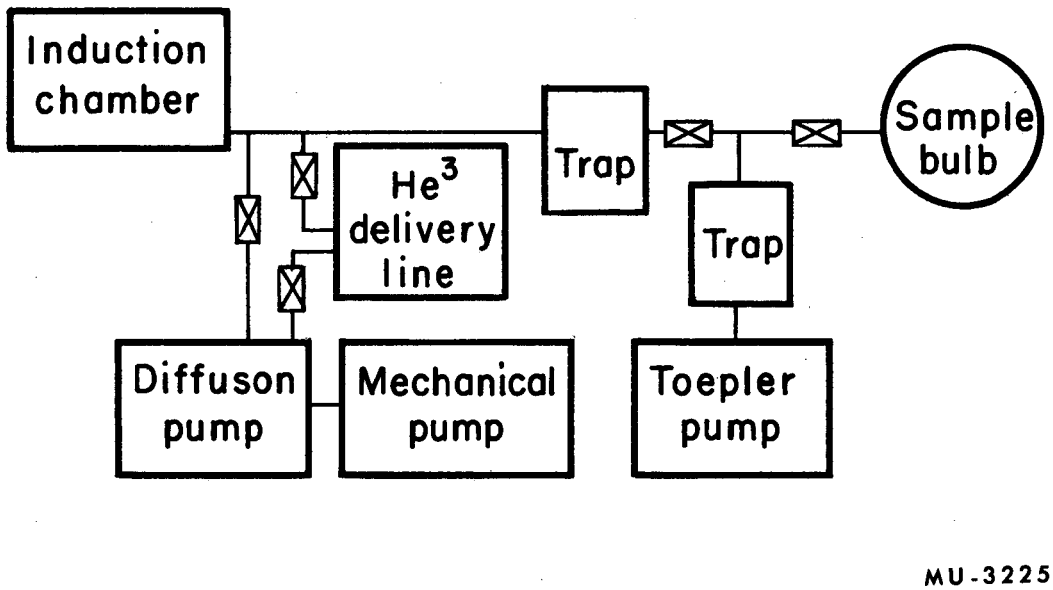

Fig. 20. Block diagram of isotope dilution system.

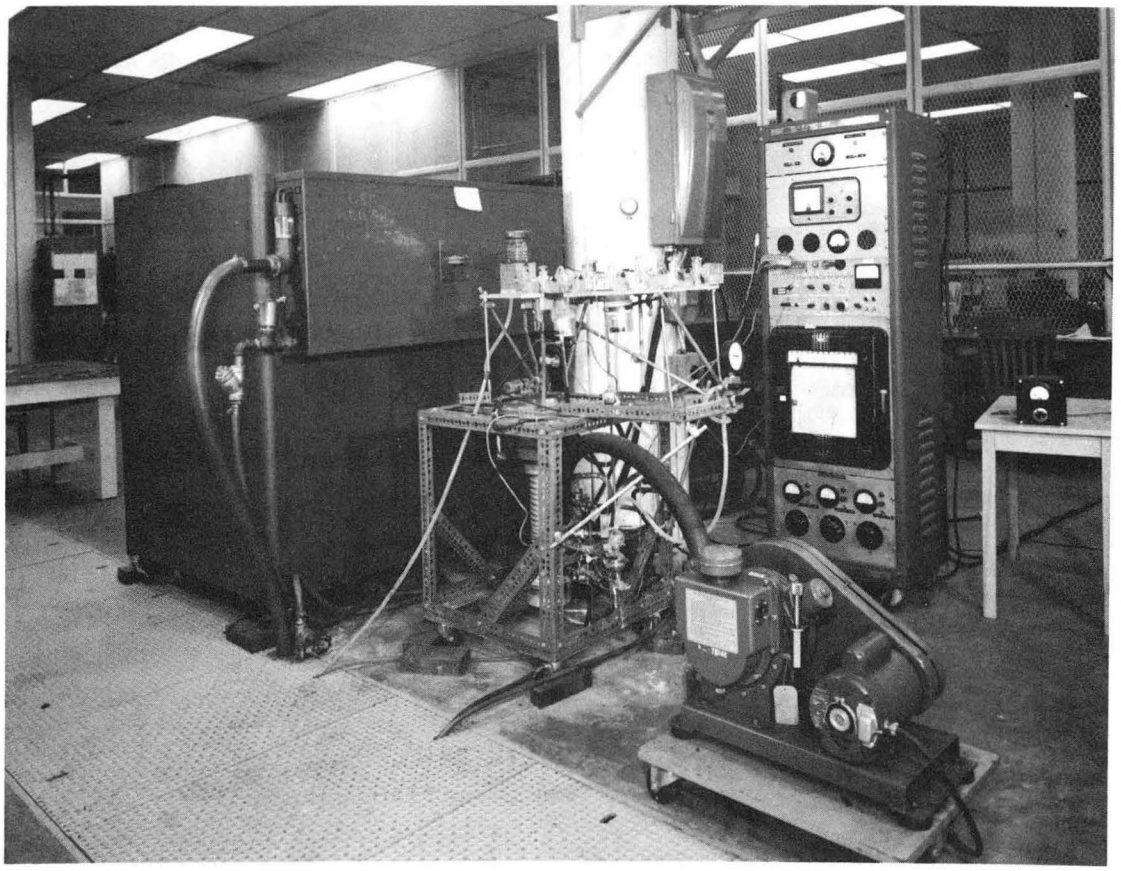

ZN-4252

Fig. 21. Side view of isotope dilution system.

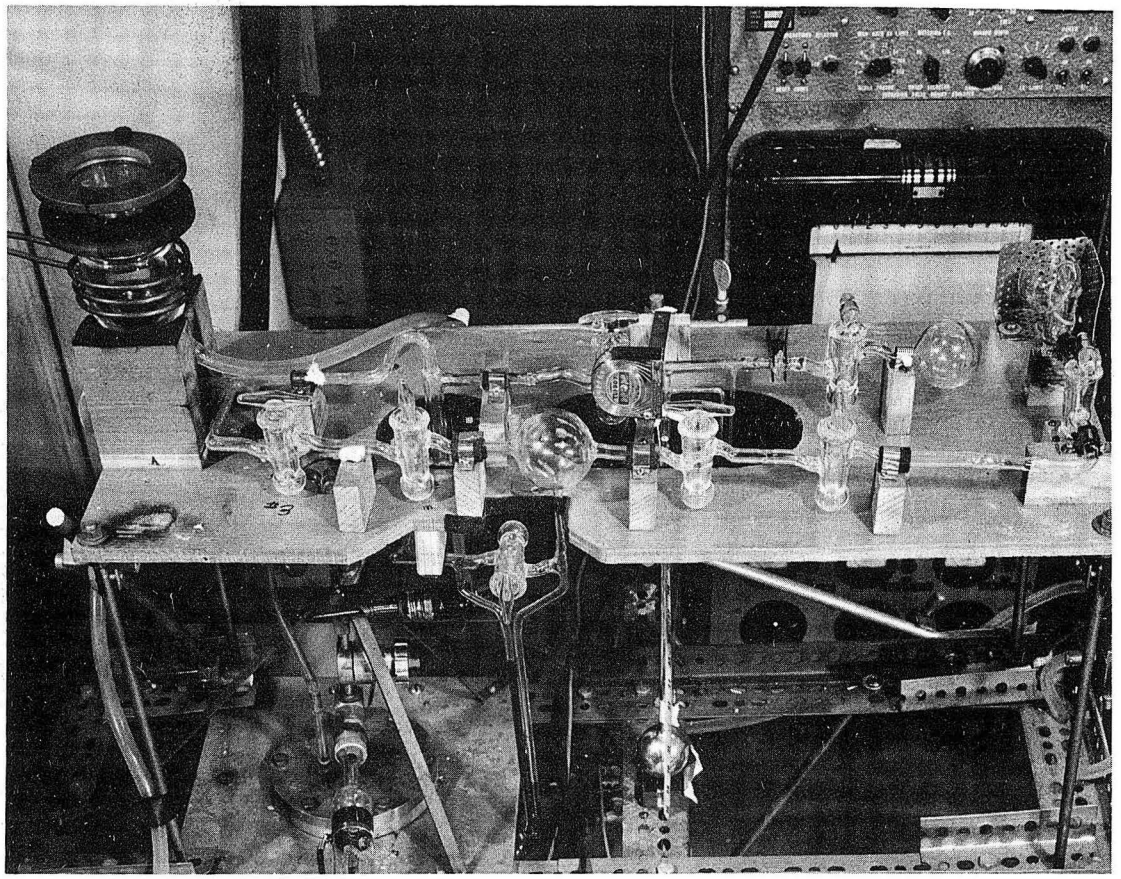

ZN-4250

Fig. 22. Top view of isotope dilution system.

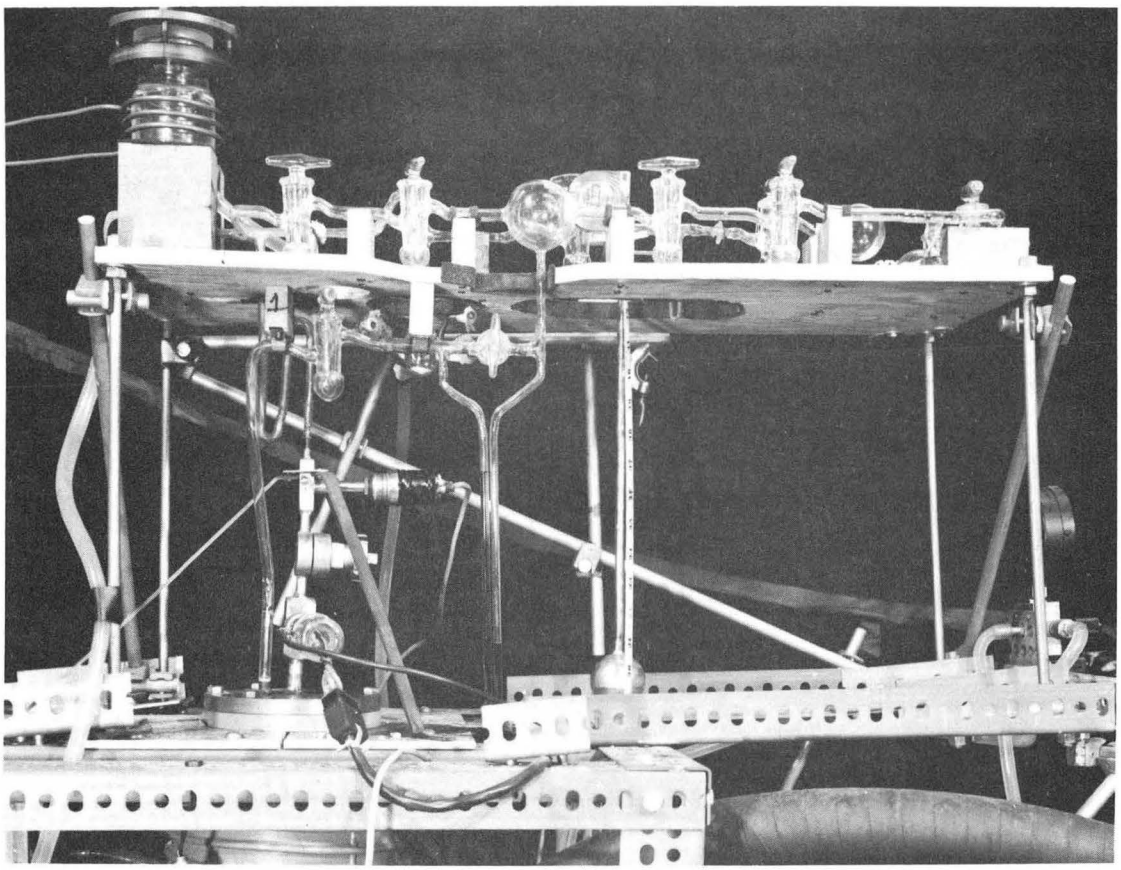

ZN-4251

Fig. 23. Complete isotope dilution system.

B. UO_2 Chemical Certification Report

The details of UO_2 powder characteristics as supplied by the manufacturer are as follows:

Table IV. Impurities on UO_2 bases, in parts per million.

Al	60.0	K	<6.0	Ti	15.0	Nb	< 4.0
B	1.2	Li	1.8	V	3.0	Pd	< 1.0
Ba	< 2.0	Mg	3.0	As	<10.0	Rb	<20.0
Be	< 0.01	Mn	40.0	Au	< 1.0	Sb	< 2.0
Ca	<10.0	Na	20.0	Bi	< 1.0	Sr	<20.0
Cd	< 0.1	Ni	40.0	Cs	<100.0	Tl	< 4.0
Co	1.0	P	<100.0	Ga	< 1.0	W	<100.0
Cr	60.0	Pb	6.0	Ge	< 0.4	Zn	< 10.0
Cu	20.0	Si	60.0	Hg	<100.0	Zr	< 20.0
Fe	600.0	Sn	< 1.0	In	<2.0	Mo	15.0

C. Mass Spectromeric Analysis

Table V. Mass-spectrometric analysis of He^3 reservoir.

He^4	0.26%
H_2O	0.10%
Air	0.07%
Acetone	0.05%
He^3	balance

Table VI. Mass-spectrometric analysis of He^3 - He^4 mixture in the sample bulb in run 7.

He^3	0.17%
He^4	1.89%
N_2	25.4%
O_2	70.0%
Ar	0.04%
H_2O	0.3%

REFERENCES

1. R. M. Barrer, Diffusion in and Through Solids (Cambridge University Press, Cambridge, 1951).
2. A. H. Booth, A Method of Calculating Fission Gas Diffusion from UO_2 Fuel and its application to the X-2-f Loop Test, Atomic Energy of Canada Ltd. Report CRDC-721, September 1957 (unpublished).
3. J. Belle, Uranium Dioxide: Properties and Nuclear Applications, U. S. Atomic Energy Commission, Washington, D. C., July 1961.
4. W. B. Lewis, The Return of Fission Products Gases to UO_2, Atomic Energy of Canada, Ltd. Report AECL-964, January 1960 (unpublished).
5. A. H. Booth and G. T. Rymer, Determination of Diffusion Constant of Fission Xenon in UO_2 Crystals and Sintered Compacts, Atomic Energy of Canada Ltd. Report AECL-692, August 1958 (unpublished).
6. H. Shaked, Diffusion of Xenon in Uranium Monocarbide Crystals (Ph. D. Thesis), University of California Lawrence Radiation Laboratory Report UCRL-10462, November 1962 (unpublished).
7. H. S. Carslaw and J. C. Jaeger, Conduction of Heat in Solids, (Oxford University Press, London, 1959), pp. 233-234.
8. J. D. Eichenberg, P. W. Frank, T. J. Kisiel, B. Lustman, and K. H. Vogel, Effects of Irradiation on Bulk Uranium Dioxide, WAPD-183, October 1957 (unpublished).

This report was prepared as an account of Government sponsored work. Neither the United States, nor the Commission, nor any person acting on behalf of the Commission:

A. Makes any warranty or representation, expressed or implied, with respect to the accuracy, completeness, or usefulness of the information contained in this report, or that the use of any information, apparatus, method, or process disclosed in this report may not infringe privately owned rights; or

B. Assumes any liabilities with respect to the use of, or for damages resulting from the use of any information, apparatus, method, or process disclosed in this report.

As used in the above, "person acting on behalf of the Commission" includes any employee or contractor of the Commission, or employee of such contractor, to the extent that such employee or contractor of the Commission, or employee of such contractor prepares, disseminates, or provides access to, any information pursuant to his employment or contract with the Commission, or his employment with such contractor.